ALUMINUM RESEARCH LABORATORIES

Technical Paper No. 2

MODEL TESTS OF LATTICED STRUCTURAL FRAMES

BY

E. C. HARTMANN
R. L. MOORE
MARSHALL HOLT

Published by

ALUMINUM COMPANY OF AMERICA
PITTSBURGH, PENNSYLVANIA

Technical Paper No. 2

Model Tests of Latticed Structural Frames

SYNOPSIS

THIS paper describes a series of beam, torsion and compression tests on twelve models of latticed frame construction. The models include riveted frames of square, rectangular and triangular cross section, braced with single-diagonal, double-diagonal and quadrangular systems of latticing. The experimental results emphasize some fundamental differences in the behavior of single- and double-angle members, show the effects of joint eccentricities upon secondary stresses and deflections, and indicate the effects of lateral bracing on the ultimate compressive strength of continuous chords. Comparisons of measured and computed stresses and deflections are presented for a number of cases to show the importance of considering the above factors in design.

INTRODUCTION

This experimental investigation was originally undertaken in connection with the design of aluminum alloy dragline booms. These booms are usually composed of continuous longitudinal chords tied together by means of some form of latticing. Although the design is based on the assumption that the boom acts principally as a compression strut, bending loads from wind, swing and dead load are also considered. In designing for minimum weight it is essential to know the relative merits of various types of latticing in relation to different combinations of loading. It is particularly important to know which types of latticing produce a minimum of secondary bending in the chords, since tests of booms in service have shown that such bending may be of serious magnitude.

In developing this program of model tests it became apparent that the results could readily be made applicable, at least qualitatively, to latticed structural frames in general, including not only dragline booms, but all frames constructed with continuous chords joined by a system of latticing. With this in mind several models not strictly representative of dragline boom construction were included because of their general structural interest.

The twelve models used in this investigation were built of Alcoa alloy 17S-T, but it should be emphasized that the results of the tests, except ultimate strengths, apply equally well to other strong aluminum alloys. Each of the models was tested under a variety of loading conditions in order to obtain experimental evidence concerning the relative merits of different types of latticing, the range of secondary stresses likely to be encountered, and other useful structural information. It is the purpose of this paper to discuss some of the more significant results obtained.

Description of Models

THE twelve models built for test were all of riveted construction, 109.5 inches in overall length. Twelve-inch panel lengths were used in at least two planes of latticing. The essential differences may be described as follows:

Frames No. 1 to 4 were of identical square section with $\frac{3}{4}$ inch by $\frac{3}{4}$ inch by $\frac{3}{32}$ inch single-angle chords and $\frac{1}{2}$ inch by $\frac{1}{2}$ inch by $\frac{1}{16}$ inch single-angle latticing. Photographs of the frames are shown in Figures 17 and 18. In Frame No. 1

the panel points in adjacent planes of latticing were staggered, while in Nos. 2, 3 and 4 the panel points coincided. The latticing at each panel point in Nos. 1, 2 and 3 was connected to the chords by a single rivet, while in No. 4 each bar had separate connections. The joint details are indicated in Figure 11. Frames No. 2 and 3 were identical except that an extra transverse cross-frame, similar to that used at the ends, was used at the mid-point of No. 3.

Frames No. 5, 6 and 7 were of square section with $\frac{3}{4}$ inch by $\frac{3}{4}$ inch by $\frac{3}{32}$ inch single-angle chords, similar to Nos. 1 to 4 but with $\frac{1}{2}$ inch by $\frac{1}{32}$ inch double diagonal straps and $\frac{1}{2}$ inch by $\frac{1}{2}$ inch by $\frac{1}{16}$ inch single-angle struts for latticing. Photographs of these frames are shown in Figures 3, 19 and 20. In Frames No. 5 and 6 the latticing at each panel point was connected to the chords by a single rivet, while in No. 7 separate connections were used for each bar. The joint details are indicated in Figure 12. Frames No. 5 and 6 were identical except that extra transverse cross-frames were used at the third points of No. 6.

Frame No. 8 was also of square section with $\frac{3}{4}$ inch by $\frac{3}{4}$ inch by $\frac{3}{32}$ inch single-angle chords but with a quadrangular system of latticing of the Vierendeel type. The lattice bars consisted of small channels of 0.060 inch thick material, $\frac{13}{16}$ inch deep with $\frac{1}{4}$ inch flanges.* Figure 12 indicates the joint details and Figures 1, 2 and 20 show photographs of the frame.

Frames No. 9 and 10 were of rectangular section with $\frac{3}{4}$ inch by $\frac{3}{4}$ inch by $\frac{3}{32}$ inch double-angle chords. Single-diagonal latticing was used in the 12-inch planes, while double diagonals with struts were used in the 18-inch planes. Figures 5 to 8 indicate the structural details. The only difference in the two frames was that the lattice bars in the 18-inch planes of No. 9 were riveted directly to the chords, while in No. 10 gusset plates were used and the working lines of all members at each joint intersected at a common point. Photographs of the frames are shown in Figure 21.

Frames No. 11 and 12 were of identical triangular section with $\frac{11}{16}$ inch by $\frac{11}{16}$ inch by $\frac{3}{32}$ inch 60° angle chords. The latticing in No. 11 consisted of $\frac{1}{2}$ inch by $\frac{1}{2}$ inch by $\frac{1}{16}$ inch single-angle diagonals with the panel points in adjacent planes staggered as in Frame No. 1. The latticing in No. 12 was composed of $\frac{1}{2}$ inch by $\frac{1}{32}$ inch double diagonal straps and $\frac{1}{2}$ inch by $\frac{1}{2}$ inch by $\frac{1}{16}$ inch single-angle struts as in No. 5. Figure 13 indicates the joint details and Figure 22 shows photographs of the frames.

TABLE I

WEIGHTS OF FRAMES

Frame No.	Weight, pounds	Frame No.	Weight, pounds	Frame No.	Weight, pounds
1	11.8	5	10.4	9	25.7
2	11.8	6	10.7	10	27.6
3	12.2	7	10.3	11	10.5
4	11.7	8	12.2	12	9.2

Table I shows the weights of the frames. The nominal dimensions and measured section elements of the members to be referred to in this paper have been included in Figures 4, 11 and 13. Table II gives a summary of the mechanical properties of the material used.

Procedure

In order to investigate the structural action of the frames under a variety of loading conditions each was subjected to a series of beam, torsion and compression tests. The loads in bending and torsion were kept well within the limits of elastic action, while those in compression were carried to ultimate failure.

The beam tests were made in a 40,000 pound capacity Amsler hydraulic testing machine using an intermediate load range. Figure 1 shows a typical set-up for one of the square frames subjected to a concentrated load at the center of a span of 108 inches. Vertical deflections were measured by means of a dial indicator, graduated to 0.001 inch, with respect to the auxiliary beam sup-

*Alcoa Die No. K-5284.

TABLE II

PROPERTIES OF MATERIAL USED FOR LATTICED STRUCTURAL FRAMES

(*Alcoa 17S-T Alloy*)

Section	Tensile Strength, lb. per sq. in.	Tensile Yield Strength (0.2% set), lb. per sq. in.	Compressive Yield Strength (0.2% set), lb. per sq. in.	Elongation in 2 Inches, per cent
¾ inch by ¾ inch by 3/32 inch—90° angle	58 800	45 400	37 200	19.0
11/16 inch by 11/16 inch by 3/32 inch—60° angle	58 500	44 800	38 300	19.8
½ inch by ½ inch by 1/16 inch—90° angle	57 800	44 400	38 400	18.0

porting the frame in the testing machine. The stress distribution in typical members was investigated by means of Huggenberger tensometers on gage lengths of ½ and 1 inch, used as indicated in Figure 1.

The torsion tests were made in a lathe, one end of the frame being supported on a plate fixed in the head of the lathe and the other similarly mounted but free to rotate on a ball-bearing center in the tail stock. Torque was applied by means of weights suspended from a beam attached to the end plate as shown in Figure 2. Measurements of twist were made using a level bar, while stresses were determined by means of tensometers.

The compression tests were made using an intermediate load range of a 300,000 pound capacity Amsler hydraulic testing machine. Three types of loading were used as indicated in Figure 3, namely:

1. Axial loads with negligible restraining moments at the ends of the frames. The bearing heads of the testing machine were provided with spherical seats, each of which rested on a nest of twenty-five hardened steel balls. The centers of rotation were at the bearing surfaces of the plates and thus at the ends of the frames. This type of loading was the one finally used for the determination of ultimate compressive strengths.

2. Eccentric loads producing a state of combined bending and direct stress with insignificant amounts of transverse shear. This loading was obtained on the various frames by displacing both ends the same amount and in the same direction from the centers of the bearing heads.

3. Oblique loads producing a state of combined bending and direct stress with rather large amounts of transverse shear. This loading was obtained on the various frames by displacing both ends equal amounts but in opposite directions from the centers of the bearing heads.

Stresses in the elastic range were measured by means of tensometers on gage lengths of ½ inch and 1 inch as in the beam and torsion tests. Values of deflection and twist were obtained by measuring with dial indicators, graduated to 0.001 inch, the movement of several points relative to auxiliary reference beams fastened to the frame of the testing machine.

Results and Discussion

THESE model tests have not only provided information concerning the relative merits of different types of framing but have emphasized several points to be considered in design. The experimental data and discussion presented in this paper pertain to three types of structural action, namely:

(*A*) *The stresses and deflections produced in the different systems of latticing.*

(*B*) *The effect of joint eccentricities on the secondary bending stresses produced in the chords.*

(*C*) *The effect of lateral bracing on the ultimate compressive strength of the chords.*

(*A*) *Lattice Bar Stresses*

In analyzing the behavior of the latticing in either the beam, torsion or compression tests under oblique loads the stress distribution in the eccentrically loaded, single-angle members seems most important from the standpoint of design. Table III and Figures 4, 5, 6 and 7 summarize a few measured stresses obtained in bars of this type and indicate the nature of the bending action produced. In the square or triangular frames, where single rivets were used at the ends of the lattice bars, the average stresses in the riveted legs ranged from 65 to 100 per cent greater than the average measured for the whole bar, yet the latter, in most cases, were within 10 per cent of the average computed values. The bending in the single-angle lattice bars of the rectangular frames having double-riveted connections was not so pronounced, but was of the same general type.

Since the shearing deflection of a plane of latticing is a function of the change in length of the individual members between connections, the high stresses in the riveted legs naturally influenced the deflections and rotations of the frames. This action is best illustrated by a comparison of the measured and computed values given in Tables IV and V. As will be noted, two sets of computed deflections and rotations have been given; one a nominal value based on average computed stresses and the other a value in which a correction has been made for certain secondary effects. In Frames No. 1, 2, 3, 4, 9*, 10* and 11 the nominal shearing deflections of the planes of latticing were increased by the ratios of the average measured stresses in the riveted legs of the angles to the average computed for the whole section. The effect of these bending stresses was most pronounced in the torsion tests since the rotations were almost entirely a function of shearing deformations in the latticing. In Table V, for instance, the measured rotations for Frames No. 1 to 4 ranged from 2.1 to 2.7 times the computed values based on average lattice bar stresses, while these same measured rotations were only 1.1

*18-inch planes.

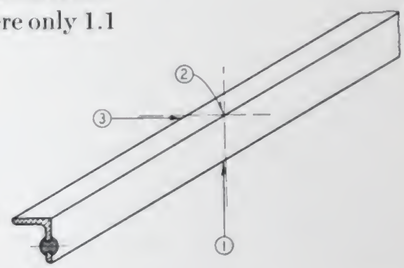

TABLE III

STRESSES IN SINGLE-ANGLE LATTICE BARS

All values are given in pounds per square inch and are averages for several sections on each bar.
The loads and torques are as given in Tables IV and V.

Frame and Type of Test	Tension Bar: Measured, Gage Line 1	Tension Bar: Measured, Gage Line 2	Tension Bar: Measured, Gage Line 3	Tension Bar: Measured, Avg. 1 & 2	Tension Bar: Measured, Avg.† 1, 2 & 3	Tension Bar: Comp.‡ Avg. 1, 2 & 3	Compression Bar: Measured, Gage Line 1	Compression Bar: Measured, Gage Line 2	Compression Bar: Measured, Gage Line 3	Compression Bar: Measured, Avg. 1 & 2	Compression Bar: Measured, Avg.† 1, 2 & 3	Compression Bar: Comp.‡ Avg. 1, 2 & 3
No. 1—Beam test	+3900	+3100	−2300	+3500	+1950	+1850	−3900	−3600	+2900	−3750	−2050	−2010
No. 1—Torsion test	+4200	+2700	−1800	+3450	+1950	+1930	−3900	−3400	+2500	−3650	−2050	−1930
No. 4—Beam test	+5600	+2900	−1300	+4200	+2500	+2220	−3900	−2700	+1700	−3300	−1900	−1850
No. 4—Torsion test	+4700	+2300	− 900	+3500	+2100	+2030	−4700	−2500	+1000	−3600	−2175	−2030
No. 9—Beam test (18-inch plane)	+5200	+4200	+1600	+4700	+3800	+3380	−5200	−4600	+ 900	−4900	−3375	−3380
No. 9—Torsion test (18-inch plane)	+4400	+3200	+1700	+3800	+3125	+2850	−3400	−4100	+ 600	−3750	−2750	−2850
No. 11—Beam test	+5000	+4100	−3400	+4550	+2450	+2030	−4600	−4500	+4700	−4550	−2225	−2030
No. 11—Torsion test	+2500	+1800	−1100	+2150	+1250	+1280	−2600	−2000	+1600	−2300	−1250	−1280

†Weighted average, gage line 2 counted twice. For example $(3900 + 2 \times 3100 - 2300) \div 4 = 1950$.
‡Secondary bending effects amounting to 8 per cent and 14 per cent of the applied shear are included for Nos. 4 and 9 respectively. All other values are nominal.

TABLE IV — SUMMARY OF DEFLECTIONS — BEAM TESTS

Frame No.	Load, pounds	Deflections in inches for 108-inch span: Measured	Computed* (1)	Computed* (2)	Ratio Measured/Computed (1)	Ratio Measured/Computed (2)	Relative Stiffness**
1	400	0.126	0.089	0.111	1.41	1.13	1.00
2	400	0.128	0.089	0.111	1.44	1.15	0.98
3	400	0.136	0.089	0.111	1.53	1.22	0.93
4	400	0.146	0.087	0.114	1.68	1.28	0.86
5	400	0.168	0.163	0.107	1.03	1.57	0.75
6	400	0.158	0.163	0.107	0.97	1.48	0.80
7	400	0.168	0.146	0.097	1.15	1.73	0.75
8	100	0.309	0.334	.....	0.92	....	0.10
9†	1000	0.118	0.110	.....	1.07	....	2.67
9††	1000	0.120	0.058	0.101	2.07	1.19	2.62
10†	1000	0.111	0.110	.....	1.01	....	2.84
10††	1000	0.093	0.063	0.083	1.48	1.12	3.39
11	400	0.176	0.100	0.148	1.76	1.19	0.72
12	400	0.152	0.193	0.115	0.79	1.32	0.83

*(1) These are nominal values based on average computed stresses. In Frames No. 5, 6, 7 and 12 the tension diagonals only were assumed to be effective.

(2) These are nominal values modified as follows: (a) In Frames No. 1, 2, 3, 10 and 11 an allowance was made for bending in the single-angle lattice bars, (b) in Frames No. 5, 6, 7 and 12 the tension and compression strap diagonals were assumed to be equally effective, (c) in Frames No. 4 and 9 (18-inch plane) an allowance was made for bending in both chords and lattice bars.

**These values are based on measured deflections, adjusted for equal loads.

†12-inch plane. ††18-inch plane.

TABLE V — SUMMARY OF ROTATIONS — TORSION TESTS

Frame No.	Torque, inch-pounds	Rotations in degrees for 108-inch length: Measured	Computed* (1)	Computed* (2)	Ratio Measured/Computed (1)	Ratio Measured/Computed (2)	Relative Stiffness**
1	2400	1.00	0.48	0.89	2.08	1.12	1.00
2	2400	1.24	0.48	0.89	2.58	1.39	0.81
3	2400	1.28	0.48	0.89	2.67	1.44	0.78
4	2400	1.19	0.44	0.90	2.70	1.32	0.84
5	2400	2.04	2.11	0.99	0.97	2.06	0.49
6	2400	1.96	2.11	0.99	0.93	1.98	0.51
7	2400	1.99	1.77	0.80	1.14	2.49	0.50
8	682	7.83	7.63	....	1.03	....	0.04
9	5400	0.86	0.34	0.72	2.53	1.19	2.63
10	5400	0.66	0.39	0.56	1.69	1.18	3.40
11	982	1.10	0.50	0.89	2.20	1.24	0.37
12	982	0.76	1.76	0.63	0.43	1.21	0.54

*(1) These are nominal values based on average computed stresses in lattice bars. In Frames No. 5, 6, 7 and 12 the tension diagonals only were assumed to be effective. The chord stresses were neglected.

(2) These are nominal values modified as follows: (a) in Frames No. 1, 2, 3, 10 and 11 an allowance was made for bending in the single-angle lattice bars, (b) in Frames No. 5, 6, 7 and 12 the tension and compression strap diagonals were assumed to be equally effective, (c) in Frames No. 4 and 9 (18-inch plane) an allowance was made for bending in both chords and lattice bars.

**These values are based on measured rotations, adjusted for equal torques.

to 1.4 times the computed values when the effect of bending in the lattice bars was included.

Although the action of the single-angle lattice bars and its effect on the behavior of the frames was quite definitely shown, the procedure to be followed in computing the stress distribution observed is not apparent. A check on the stresses for the type of member shown in Figure 4, made by assuming the bars to act as eccentrically loaded, pin-ended members under combined bending and direct stress, gave maximum values almost double those measured, indicating that the bars were not pin-ended and that the moments could not be computed directly from the joint eccentricities given. It was found, however, that if all the bending was assumed to occur about the axis parallel to the riveted leg, as is suggested by the distribution diagrams shown in Figure 4, a fair check on the measured stresses could be obtained.

The computation of the stresses in the single-angle lattice bars of Frame No. 9 was further complicated by secondary bending moments resulting from both the rigidity of the joints and the eccentricity of framing. No satisfactory general method was found for calculating the measured stress distribution in these members although a fair agreement between average measured and computed values was obtained by assuming the shear to be equally divided between the tension and compression diagonals. Actually the average tension was somewhat higher than the average compression.

Figures 6 and 8 show the comparatively uniform stress distribution found in the double-angle lattice bars of Frames No. 9 and 10. Not only were the average measured stresses in satisfactory agreement with those computed but the maximum individual values were only about 30 per cent higher than computed, a distribution in marked contrast to that observed in the single-angle bars. The stresses in the outstanding legs of the angles near the gusset plates were all somewhat low but this seems to be a characteristic behavior of members loaded through one leg. Table IV shows a good agreement between the measured and computed beam deflections of Nos. 9 and 10 in the 12-inch planes, emphasizing the merits of double-angle over single-angle latticing as far as the determinate action of such framing is concerned.

In the foregoing discussion of the behavior of single- and double-angle lattice bars, experimental data have been taken from both the beam and torsion tests. Although the analysis of the beam tests was made according to conventional methods, some explanation may be helpful concerning the analysis of the torsion tests. The total torque was assumed to be resisted by separate shearing forces acting on each plane of latticing, the magnitudes of which were proportional to the depths of the frames. For the rectangular frames the shearing forces in the 18-inch planes were 1.5 times those in the 12-inch planes and for the square and triangular frames the shearing forces on each plane were equal. The magnitudes of these separate shearing forces were so adjusted that the total moment of the individual forces about the center of rotation was equal to the total torque. The rotations of the square and triangular frames were computed by dividing the shearing deflection of a plane of latticing by the distance from the center of rotation. In the case of the rectangular frames the average of the rotations computed for the 12-inch and 18-inch planes of latticing was used. As has already been indicated, the shearing deflections of the planes of single-angle latticing were increased to allow for the bending observed in those members.

The behavior of the double-diagonal strap latticing of Frames No. 5, 6, 7 and 12 was influenced by the initial tensions purposely introduced in the diagonals during fabrication to keep them taut, hence it was not possible to subject these frames to a very exact analysis. The measured stresses in Nos. 5 and 7, for instance, indicated that about 80 per cent of the total shear was carried by the tension diagonals, while in the case of No. 12 about 60 per cent of the shear was carried in this manner. The exact distribution depended, of course, both upon the initial tensions and the magnitude of the loads applied. The load-deflection and torque-twist curves shown for the different frames in Figures 9 and 10 indicate that those having double-diagonal strap latticing were the only ones for which linear load-deflection relations were not obtained.

Tables IV and V give values of measured and computed deflections and rotations for the frames having strap-diagonal latticing. Two computed

values have been included, one based on the assumption that the tension diagonals only were operative and the other on the assumption that the tension and compression diagonals were equally effective. From the relative magnitudes of the measured and computed values an indication of the proportion of the shear resisted by the compressive straps can be obtained.

The tests on Frame No. 8 clearly emphasized the weaknesses of quadrangular framing as compared to the other types of latticing used. In the beam test, for instance, the measured deflection was about ten times that found for No. 1 under the same load. In the torsion test the difference was even more pronounced, the rotation being approximately twenty-five times that found for No. 1. An analysis of No. 8 by the method of slope deflections* indicated, however, a very close agreement between the measured and computed stresses and deflections, much better, in fact, than found for some of the frames having diagonal latticing.

(*B*) *Chord Stresses, Beam and Torsion Tests*

Figures 5 to 8 and 11 to 13 show some interesting examples of the stress distribution found in the chords of the different models. Since the highest ratios of maximum to average stress were found in the beam tests, these have been used in most cases to illustrate the significant types of action observed. Although the average measured and computed values were in fair agreement, it is at once apparent that the stress distribution on most of the sections investigated was far from uniform. The maximum individual stresses in Frames No. 4 and 9, having the largest eccentricities at the joints, were 2.7 and 4.9 times the average computed values respectively. Stresses in the other frames were as high as 1.8 times the average. These data indicate that for certain types of framing the matter of secondary stresses may be of considerably more importance than is generally recognized in design.

As will be noted, Figures 5 to 8 and 11 to 13 show both measured and computed chord stresses. The latter values have been included in an attempt to show how closely the behavior of such types of framing may be predicted by ordinary methods of analysis. It is obvious from the stress-distribution diagrams and the foregoing discussion concerning the stresses and deflections found in the different lattice systems that a simple computation of primary stresses is not always adequate.

In the case of the single-angle chords involving diagonal latticing the joint eccentricities were apparently responsible for most of the secondary stresses observed. In view of the single-riveted connections used, joint rigidities were neglected in the analysis even though the chords were continuous. Figure 14 shows the analysis made for the secondary bending moments in the chords of Frame No. 1. The procedure, which was essentially the same for all single-angle chords, with the exception of those in No. 8, may be described as follows:

1. The bending moments due to joint eccentricities were determined for each panel point. Moments about Axes 1-1 and 2-2, parallel to the legs of the angles, were selected for purpose of illustration, although a more direct solution would have been obtained if the moments about the principal axes had been determined since these were the ones finally used.

2. The relative stiffness factors or K values were determined for each panel length.†

3. The moments applied at each joint were distributed among the chord segments in proportion to the relative stiffness factors, K.

4. The final moments for the sections in question were resolved into components about the principal axes (Axes 3-3 and 4-4 in Figure 11) and the bending stresses computed by the flexure formula.‡

As previously indicated, the moments in Frame No. 8 were determined by the method of slope deflections. The computation of chord stresses, however, was made according to the same procedure as indicated in Item 4 above.

*See "*Analysis of Statically Indeterminate Structures by the Slope Deflection Method*," by W. M. WILSON, F. E. RICHART and CAMILLO WEISS, Bulletin No. 108, University of Illinois.

†See "*Continuous Frames of Reinforced Concrete*," by HARDY CROSS and N. D. MORGAN (John Wiley and Sons, 1932), p. 119.

‡See "*Resistance of Materials*," by F. B. SEELY (John Wiley and Sons, 1935), Chapter XV on Unsymmetrical Bending.

The agreement obtained between the measured and computed stresses in the single-angle chords, shown in Figures 11, 12 and 13 was sufficiently good in most cases to justify the methods of analysis used. The results shown in Figure 11 for the tension chords of Frames No. 1, 2 and 4 and in Figure 12 for both chords of Frame No. 8 were the best examples obtained. The stresses in the compression chords of Nos. 1, 2 and 4 were probably influenced somewhat by local distortions at the point of load application, while this factor combined with the uncertainty of the distribution of shear in the double diagonal straps complicated the analysis of Frames No. 5 and 7. The computed values for the latter, shown in Figure 12, were based on the assumption that 80 per cent of the shear was carried by the tension diagonals, a distribution supported by the measured lattice bar stresses. In the case of Frame No. 12, it was indicated that about 60 per cent of the shear was carried by the tension diagonals and the computations were based on such a distribution.

The most important observation made from the tests on the single-angle chords was that the secondary bending moments could readily be determined from the eccentricities of framing and the stresses computed with reasonable accuracy by the ordinary flexure formula. Since the problem was one involving unsymmetrical bending, the moments about the principal axes rather than about the axes parallel to the legs of the chord angles were used.

Figures 5 to 8 show the measured and computed stress distribution in the double-angle chords of Frames No. 9 and 10. The marked difference in the range of secondary stresses observed in the 18-inch planes may be attributed entirely to the effect of joint eccentricities since in all other respects the frames and the loads to which they were subjected were identical. The maximum stresses in No. 10 in which the latticing was framed into gusset plates with the working lines of all members at each joint intersecting at a common point were less than one half those found in No. 9 in which the latticing was riveted directly to the chords. From the agreement obtained between measured and computed values it is apparent, however, that both types of action were reasonably determinate from the standpoint of analysis. It is obvious from the stress distribution shown for No. 9 that the two angles composing the chord sections did not act as a unit. The same was probably true for No. 10 although the bending moments were too small to indicate such a behavior. The use of additional stitch rivets between the angles of the chords undoubtedly would have produced a more unified action and lower bending stresses.

Figure 15 shows the bending moment curves computed for the chords of Frame No. 9. The moments due to the rigidity of the joints, obtained by the method of moment distribution,* were assumed to be the same as those computed for No. 10 in which the members at each joint had a common point of intersection. In evaluating the relative stiffness of the different members the moment of inertia of the chord section was taken to be twice that of a single chord angle, i.e., integral action between the two angles of a chord was not assumed. In computing the primary stresses from which the angle changes were determined the shear was equally distributed between the tension and compression diagonals.

As indicated in Figure 15, the moments due to the rigidity of the joints were of small magnitude in comparison with those resulting from joint eccentricities. The latter were obtained by considering the chord to act as a continuous beam supported at the panel points and subjected to loads equal to the vertical components of the lattice bar reactions. The fixed-end moments at the panel points were computed and distributed to the members at each joint in proportion to their relative stiffnesses.

The bending stresses in the chords of No. 9 were computed from the sum of the moments shown in Figure 15, while in the case of No. 10 the moments due to the rigidity of the joints were the only ones considered. In both frames the two angles in each chord were assumed to act separately, each resisting one-half of the total bending moment. Since the problem was one involving symmetrical bending, the axes parallel to the legs of the angles were used.

In Frame No. 9 the secondary bending moments resulting from joint eccentricities were of

*See "*Continuous Frames of Reinforced Concrete*," by Hardy Cross and N. D. Morgan (John Wiley and Sons, 1932), p. 242.

sufficient magnitude to influence materially the beam deflections in the 18-inch planes. For a distance at each panel point equal to the eccentricity of the lattice bar connections there were no diagonals effective and the shear on the frame was resisted entirely by bending in the chords. The total deflection resulting from this action was computed to be over one-third the nominal value given in Table IV and almost enough to account for the difference in the measured deflections of Nos. 9 and 10. The shear deflection or offset at each panel point was obtained by multiplying the slope of the chord as computed from the bending moment curves in Figure 15 by the distance between lattice bar connections.

A second point of interest in connection with the high secondary stresses in No. 9 was their effect on the primary stresses. The shear carried by the chords as a result of the bending moments shown in Figure 15 was sufficient to increase the average computed lattice bar stresses about 14 per cent over their nominal value. A similar effect was found in the case of Frame No. 4 where the lattice bar stresses were increased about 8 per cent. The eccentricities in the other square frames having single-diagonal latticing were such as to decrease rather than increase the lattice bar stresses, the effect amounting to about 5 per cent.

Figure 6 shows the stresses measured in the chords of Frame No. 9 in the torsion test. As far as the effect of the joint eccentricities in the 18-inch planes of latticing was concerned, the behavior was essentially the same as found in the beam test. The secondary bending moments were computed as a function of the shear in the same manner as described in Figure 15. The computed direct stresses in the chords, which were either zero or relatively small in all the torsion tests, were obtained by summing up the longitudinal components of the shear introduced by the lattice bars in adjacent planes.

Figure 8 shows the stress distribution found in the chords of Frame No. 10, loaded as a beam in the 12-inch planes. The maximum chord stresses were only about 20 per cent greater than the average computed and the measured beam deflection, as previously pointed out in connection with the action of the double-angle lattice bars, was within a few per cent of the nominal computed value.

Figure 16 shows the secondary bending moments computed for the chords of No. 10. Those resulting from the rigidity of the joints were computed by the method of moment distribution previously referred to, while those due to joint eccentricities were obtained by the method illustrated in Figure 14. The only variation from the procedure indicated in the latter figure was that the moments introduced at each joint were distributed to the lattice bars as well as to the chords. As is shown in Figure 8, the secondary stresses computed from the moments obtained were in satisfactory agreement with those measured. There were no appreciable bending stresses indicated for the lattice bars since the moments resulting from the rigidity of the joints were of about equal magnitude but of opposite sign from those due to the eccentricity of framing.

In the discussion thus far, emphasis has been placed upon the two most significant types of action observed in the beam and torsion tests: (1) the comparative behavior of single- and double-angle lattice bars and (2) the effect of joint eccentricities on the secondary stresses produced in the chords. Although a number of the same characteristics of behavior were noted in the compression tests, the principal object of the latter was to investigate the effect of lateral bracing on the ultimate compressive strength of the chords.

(C) *Chord Stresses, Compression Tests*

The data given in Table VI indicate the nature of the stress distribution found in the chords in the compression tests. The average measured stresses in all cases were in satisfactory agreement with those computed, while the maximum values, omitting those found in Frame No. 8, ranged as high as 1.36 times the average. In view of the nature of the secondary stresses observed in the chords in the beam and torsion tests, it would be expected that the highest ratios of maximum to average stress in compression would be found under the oblique loadings, yet such was not the case. In nine of the eleven frames the highest stress ratios were found under the axial or eccentric loadings. From the small differences indicated in Table VI, however, it may be concluded that the secondary stresses produced in the chords by any

TABLE VI

SUMMARY OF CHORD STRESSES—COMPRESSION TESTS

All stresses are given in pounds per square inch for loads corresponding to an average chord stress, P/A, of 8000 pounds per square inch

	AXIAL LOADS, e = 0				ECCENTRIC LOADS, e = 3 INCHES				OBLIQUE LOADS, e = 2 INCHES AT ENDS			
FRAME NO. (1)	Maximum Measured (2)	Average Measured (3)	Average Computed (4)	Ratio (2)/(4) (5)	Maximum Measured (6)	Average Measured (7)	Average Computed (Concave Side) (8)	Ratio (6)/(8) (9)	Maximum Measured (10)	Average Measured (11)	Average Computed (Concave Side) (12)	Ratio (10)/(12) (13)
1	8 800	8 200	8 000	1.10	13 100	11 800	12 150	1.08	11 200	10 600	10 760	1.04
2	9 600	8 300	8 000	1.20	14 100	12 500	12 150	1.16	11 800	10 600	10 760	1.09
3	9 400	8 200	8 000	1.17	14 600	12 300	12 150	1.20	12 000	10 900	10 760	1.11
4	8 800	8 200	8 000	1.10	13 700	12 200	12 150	1.13	12 100	10 800	10 760	1.12
5	8 900	8 100	8 000	1.11	15 200	12 400	12 150	1.25	12 400	10 700	10 760	1.15
6	8 800	7 700	8 000	1.10	14 300	11 700	12 150	1.18	11 400	9 900	10 760	1.06
7	10 400	7 800	8 000	1.30	16 500	11 800	12 150	1.36	12 100	10 400	10 760	1.13
8	13 400	....	8 000	1.67	....	....	....	.....	....	....	....	.....
9	9 400	8 100	8 000	1.18	13 500[a]	11 200	12 150	1.11	9 600[a]	8 400	8 460	1.14
10	8 700	7 500	8 000	1.09	13 200[a]	11 300	12 150	1.08	9 500[a]	8 400	8 460	1.12
11	8 800	7 800	8 000	1.10	12 600[b]	11 400	11 570	1.09	12 100[b]	11 200	11 570	1.04
11	....	....	....	.....	12 000[c]	10 800	11 100	1.08	11 400[c]	10 600	11 100	1.02
12	8 100	7 600	8 000	1.01	11 600[b]	11 000	11 570	1.00	14 100[b]	10 200	11 570	1.22
12	....	....	....	.....	13 200[c]	11 000	11 100	1.19	12 300[c]	10 300	11 100	1.11

a—Axis of bending parallel to long sides, e = 3 inches.
b—Axis of bending parallel to one side, e = 2 inches.
c—Axis of bending normal to one side, e = 2 inches.

Average measured stresses given for sections showing maximum measured values. Stresses under oblique loads measured in end panels of all frames except Nos. 9 and 10, where values were taken on a section 9 inches from the center.
Average computed stress = $P/A\ (1+ec/r^2)$ where:
e = distance between load line and neutral axis of section, inches.
c = distance between center of gravity of chords and neutral axis of section, inches.
r = radius of gyration of section, inches.

one of the three types of compressive loads were not of serious magnitude.

Although no lattice bar stresses have been given for the compression tests, it was found that the double-diagonal systems were effective in carrying part of the applied loads. In Frames No. 5, 6, 7 and 12 it was noted that all the strap diagonals, which originally had some initial tension, buckled laterally in the early stages of the tests. Moreover, the average measured and computed chord stresses given in Table VI for these frames are consistent in most cases with the fact that participation stresses were developed in the latticing. A similar observation was made in the case of Frames No. 9 and 10 where double-diagonal latticing was used in the 18-inch planes. In five of the six cases investigated on these frames the average measured chord stresses were less than the average computed. For the case of axial loads on Frame No. 10 the double-diagonal lattice bars were computed to carry about 8 per cent of the total load.* The measured stresses in the chords of this frame indicated that about 6 per cent of the total load was carried by the double-diagonal lattice bars.

Table VII gives a summary of the lateral de-

*For method of computation see "*Modern Framed Structures, Part II*," by Johnson, Bryan and Turneaure (John Wiley and Sons, 1911), p. 367.

flections measured in the compression tests under eccentric loads. Since only small shearing stresses and deformations were developed in the latticing, a very satisfactory agreement between measured and computed deflections was obtained. In the beam and torsion tests, it will be recalled, the difficulty encountered in computing deflections and rotations was due principally to the action of the single-angle lattice bars under transverse shears.

Table VIII gives a summary of the maximum loads carried by the frames and the corresponding ultimate compressive strengths of the chords. Figures 17 to 22 inclusive show the frames after failure. Several observations were made which have an important bearing upon the influence of the latticing used. Frame No. 1 was considerably stronger than any of the other square frames because the panel points in adjacent planes were staggered and the lateral restraint thus provided prevented failure of the chord segments about the axis of least stiffness. Where the panel points in adjacent planes coincided, however, as was the case in Nos. 2 to 7, there was nothing to prevent the chord segments from failing in their weakest direction and hence lower strengths were obtained. Figure 17 shows these two types of column action as found in Frames No. 1 and 2.

As noted previously, the double-diagonal strap latticing in Frames No. 5, 6, 7 and 12 buckled laterally in the early stages of the compression tests, leaving only the angle struts effective as bracing. With the straps inoperative the lattice system was apparently reduced to a quadrangular type with single-rivet connections at the joints of the struts and chords. For increasing loads, however, the frames remained quite straight and free from twist until collapse. The action was entirely different from that observed for No. 8, which although it had rigid joints, failed by twisting at a much lower load.

Frames No. 9 and 10 which had a slenderness ratio for the chord segments less than for the other frames naturally developed the highest average stresses at failure. Figure 21 shows that fail-

TABLE VII

SUMMARY OF LATERAL DEFLECTIONS COMPRESSION TESTS

Eccentricity, e, equals 3 inches except as noted.

Frame No.	Load,† pounds	Deflections in inches for 109.5-inch length	
		Measured	Computed
1	4 000	0.112	0.110
2	4 000	0.112	0.110
3	4 000	0.104	0.110
4	4 000	0.104	0.110
5	4 000	0.120	0.110
6	4 000	0.118	0.110
7	4 000	0.104	0.110
9	8 000	0.101	0.110
10	8 000	0.098	0.110
11	3 410	0.056[a]	0.061
		0.058[b]	0.061
12	3 410	0.056[a]	0.061
		0.051[b]	0.061

†—These loads correspond to an average chord stress, P/A, of 8000 pounds per square inch.
a—Axis of bending parallel to one side, e = 2 inches.
b—Axis of bending normal to one side, e = 2 inches.

TABLE VIII

SUMMARY OF ULTIMATE STRENGTHS COMPRESSION TESTS

All Loads Applied Axially

Frame No.	Maximum Load, pounds	Ultimate Compressive Strength, lb. per sq. in.	Slenderness Ratio of Chord Segment, (L/r)	Effective Slenderness Ratio Coefficient, K*
1	11 100	22 200	85.3	0.73
2	8 750	17 500	85.3	0.87
3	8 450	16 900	85.3	0.89
4	8 920	17 840	85.3	0.86
5	7 540	15 080	85.3	0.95
6	8 150	16 300	85.3	0.91
7	8 650	17 300	85.3	0.88
8	5 600	11 200	85.3	. . .
9	25 400	25 400	52.3	1.00
10	26 720	26 720	52.3	0.93
11	10 810	25 380	67.0	0.79
12	9 370	22 000	67.0	0.94

*Determined from curve of column strengths for chord sections, shown in Figure 23, and the slenderness ratio, L/r, of the chord segments.

ure occurred by buckling of the chords in the 18-inch planes. It should be pointed out that the slenderness ratio (L/r) of the chord segments acting as a unit and bending in this direction was 52.3, whereas the slenderness ratio in the 12-inch planes was 54.8. The direction of the failure indicates that the effective slenderness ratio (KL/r) was greater in the 18-inch planes. Lack of integral action of the two angles of the chords was no doubt responsible for this condition.

The ultimate strengths developed in the 60° angle chords of Frames No. 11 and 12 indicated the same fundamental difference in behavior as found between No. 1 and the other square frames. The strength of No. 11, having the panel points staggered in adjacent planes of latticing, was 15 per cent greater than found for No. 12 in which the panel points coincided. Figure 22 shows the failures obtained in these two frames.

The values of effective slenderness ratio coefficient, K*, given in Table VIII, were computed from the ultimate compressive strengths of the frames and the column strength data given in Figure 23. A value of K=1.0 indicates an effect equivalent to round or hinged ends, while a value of K=0.5 corresponds to complete fixity at the panel points. The values of the coefficient indicating the greatest restraint at the joints were found for Nos. 1 and 11 in which the panel points in adjacent planes of latticing were staggered. Since the axis about which the chords of these frames failed was not known, the slenderness ratios were arbitrarily based upon the least radii of gyration for the sections. The same procedure was used for all the single-angle chords with the result that the values of K obtained indicated, in some measure, the relative merits of the different types of latticing as far as the ultimate compressive strength of these frames was concerned. In the case of the double-angle chords in Nos. 9 and 10 the slenderness ratio was based upon an 18-inch panel length and the corresponding radius of gyration for the section, assuming integral action of the two angles. The values of K computed on such a basis were probably higher than would have been found had the true nature of the chord action been known but they are satisfactory for comparative purposes. As will be noted, the greatest restraint was indicated for the panel points of No. 10 where gusset plates were used in the 18-inch planes.

*The term, K, as used in connection with column strengths, indicates the effective slenderness ratio coefficient and has a different meaning than when used in connection with the calculation of secondary stresses where it is a stiffness factor, I/L.

In order to obtain some definite information on the action of double-angle chords as influenced by the spacing of stitch rivets, auxiliary frames 37.5 inches long, containing two 18-inch panels, were taken from the straight portions of Frames No. 9 and 10 after they had been tested to failure. One short specimen was cut from No. 9, designated as No. 9A, and two were cut from No. 10, designated as Nos. 10A and 10B. End frames were inserted at the cut sections and additional stitch rivets added to the chords of Nos. 9A and 10A to reduce the spacing to 1½ inches. The spacing of the stitch rivets in No. 10B was left at 5¼ inches as in the original frame.

The tests on these auxiliary frames were made in the same manner as previously described for axial loads except that the bearing plates were fitted with plain instead of ball-bearing spherical seats. Strain measurements, made with Huggenberger tensometers as before, indicated that the load was quite uniformly distributed among the four chords. Figure 24 shows the failures obtained.

The compressive strengths developed by the auxiliary frames are given in Table IX along with the strengths of Frames No. 9 and 10 from which they were cut. The effect of the length of specimen is indicated by a comparison of the results obtained on Frames No. 10 and 10B. Although both failed by bending in the 18-inch planes, the shorter specimen was 10 per cent stronger. This increased strength probably resulted from the fact that in No. 10B one end of each chord segment in the two 18-inch panel lengths was restrained against rotation by the bearing heads of the testing machine, whereas in No. 10 the ends of the interior panel lengths were restrained only by the latticing and the continuity of the chords. The indicated effective slenderness ratio coefficient for Frame No. 10B was 0.77.

The effect of the stitch-rivet spacing upon the strength of the chords is indicated by a comparison of the results obtained on Frames No. 10A and 10B. Frame No. 10A, with a rivet spacing equal to 1½ inches, was about 5 per cent stronger than

No. 10B, which had the original spacing of $5\frac{1}{4}$ inches. Although this difference in strength was not very great, it is significant to note, as shown in Figure 24, that No. 10A failed by bending in the 12-inch planes. Apparently the stitch-rivet spacing of $1\frac{1}{2}$ inches in No. 10A was small enough to produce substantially integral action of the chord angles and to produce failure in the direction that would normally be predicted from a consideration of the relative slenderness ratios.

The strength developed by Frame No. 10A indicates an effective slenderness ratio coefficient equal to 0.69. Inasmuch as the center one of the three 12-inch panel lengths showed the first signs of failure, the length of the specimen had a smaller effect on the strength developed by this specimen than was the case with Frame No. 10B which failed in the 18-inch planes. Frame No. 9A failed in the same manner as did Frame No. 10A and developed practically the same strength.

TABLE IX

SUMMARY OF ULTIMATE STRENGTHS—AUXILIARY COMPRESSION TESTS

All loads applied axially

Frame No.	Length, inches	Number of 18-inch Panel Lengths	Spacing of Stitch Rivets, inches	Maximum Load, pounds	Ultimate Compressive Strength, lb. per sq. in.	Effective Slenderness Ratio Coefficient, K*	Direction of Failure of Segments
9	109.5	6	$5\frac{1}{4}$	25 400	25 400	1.00	18-inch plane
9A	37.5	2	$1\frac{1}{2}$	30 930	30 930	0.69	12-inch plane
10	109.5	6	$5\frac{1}{4}$	26 720	26 720	0.93	18-inch plane
10A	37.5	2	$1\frac{1}{2}$	31 000	31 000	0.69	12-inch plane
10B	37.5	2	$5\frac{1}{4}$	29 400	29 400	0.77	18-inch plane

Frames No. 9 and 10 tested with ball-bearing spherical seats.
Frames No. 9A, 10A and 10B tested with plain spherical seats.
*Determined from curve of column strengths for chord sections shown in Figure 23, and the slenderness ratio, L/r, of the chord segments.

Summary of Results

In summarizing the results of this model study the following points should be emphasized:

1. The maximum stresses developed in the single-angle lattice bars ranged from two to three times the average, while the bending produced in these members was sufficient in some cases to increase the shearing deflections of the frames almost 100 per cent over the nominal computed values. The stresses and deflections found in the planes having double-angle lattice bars, however, were in very close agreement with those computed.

2. The frames with single-angle latticing deflected less under transverse shears than did those with strap-diagonal latticing, except in the case of Frame No. 12 where there was considerable initial tension in the straps.

3. The quadrangular bracing used in Frame No. 8 was the least efficient of all the different types investigated. The deflection in the beam test, for instance, was about ten times that observed for No. 1 under the same load, yet No. 8 was the heavier of the two frames.

4. The action of the frames with double-diagonal strap latticing was indeterminate from the standpoint of calculation because of the indefinite initial tension in the straps. The load-deflection and torque-twist curves obtained for Nos. 5, 6, 7 and 12 were not straight lines because the

stresses in the compressive straps were high enough to relieve the initial tension in some straps. In the compression tests the straps buckled laterally, apparently becoming ineffective, but there appeared to be no tendency for the specimens to deflect or twist because of the reduced rigidity. The double-diagonal latticing of Frames No. 9 and 10 was apparently effective at all times.

5. The secondary stresses produced in the single-angle chords in the beam and torsion tests were due principally to the eccentricities of framing. A rather close check between measured and computed values was obtained by treating the problem as one of unsymmetrical bending. The secondary bending moments were resolved into components parallel to the principal axes and the stresses computed by means of the ordinary flexure formula.

6. The secondary stresses in the double-angle chords in the beam and torsion tests resulted both from the rigidity of the joints and the eccentricities of framing. In Frame No. 9 the secondary stresses were of such magnitude as to have an appreciable influence upon the primary stresses and deflections. The stress distribution measured in this frame indicated that the two angles of the chord acted separately rather than as a unit. A closer spacing of stitch rivets would undoubtedly have produced a more unified action and lower secondary stresses.

7. For the frames with diagonal bracing, the maximum stresses measured in the chords in the compression tests under axial, eccentric or oblique loads did not exceed the average computed value by more than 36 per cent.

8. The most effective framing, as far as the ultimate compressive strength of the single-angle chords was concerned, was that found in Frames No. 1 and 11 where the panel points in adjacent planes of latticing were staggered. These frames carried from 15 to 47 per cent more load than those in which the panel points in adjacent planes coincided. In the latter group, where there was no question concerning the axis about which the chords failed, the end fixity at the panel points was estimated to be only about 20 per cent ($K=0.9$).

9. The highest ultimate strengths in compression were obtained on the double-angle chords of Frames No. 9 and 10, where the effective radius of gyration was greater than for the single-angle members. Failure of the chord members in these tests was in the direction of the 18-inch planes even though the slenderness ratio, assuming integral action of the two angles, was greater in the direction of the 12-inch planes.

10. In the auxiliary tests on short lengths of Frames No. 9 and 10, with the spacing of stitch rivets decreased from the original 5¼ inches to 1½ inches, the chords buckled in the direction of the 12-inch planes as would be predicted from the relative slenderness ratios. The ultimate loads in these tests indicated an end restraint of about 62 per cent ($K=0.69$).

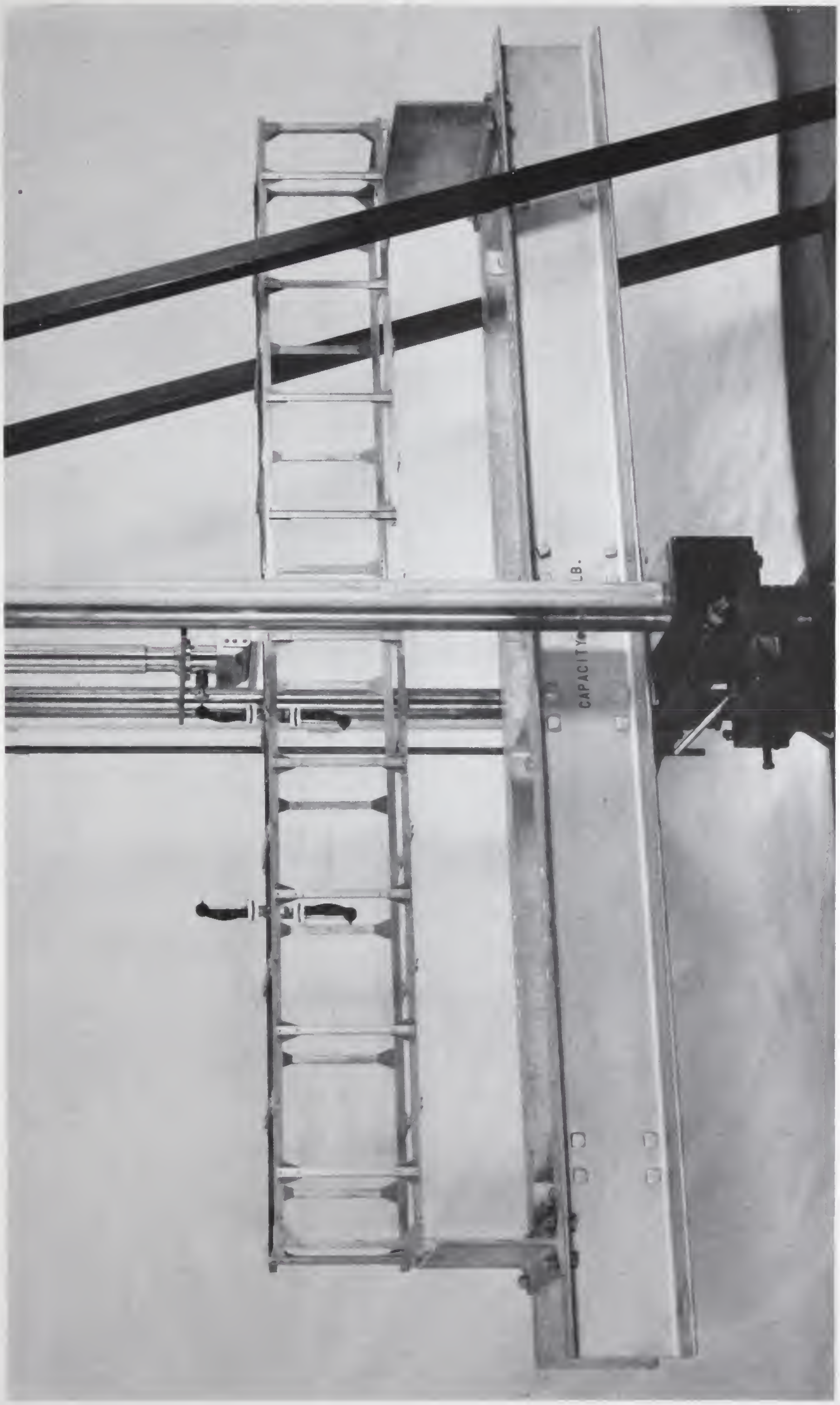

Figure 1. Beam Test on Frame No. 8.

FIGURE 2. TORSION TEST ON FRAME NO. 8.

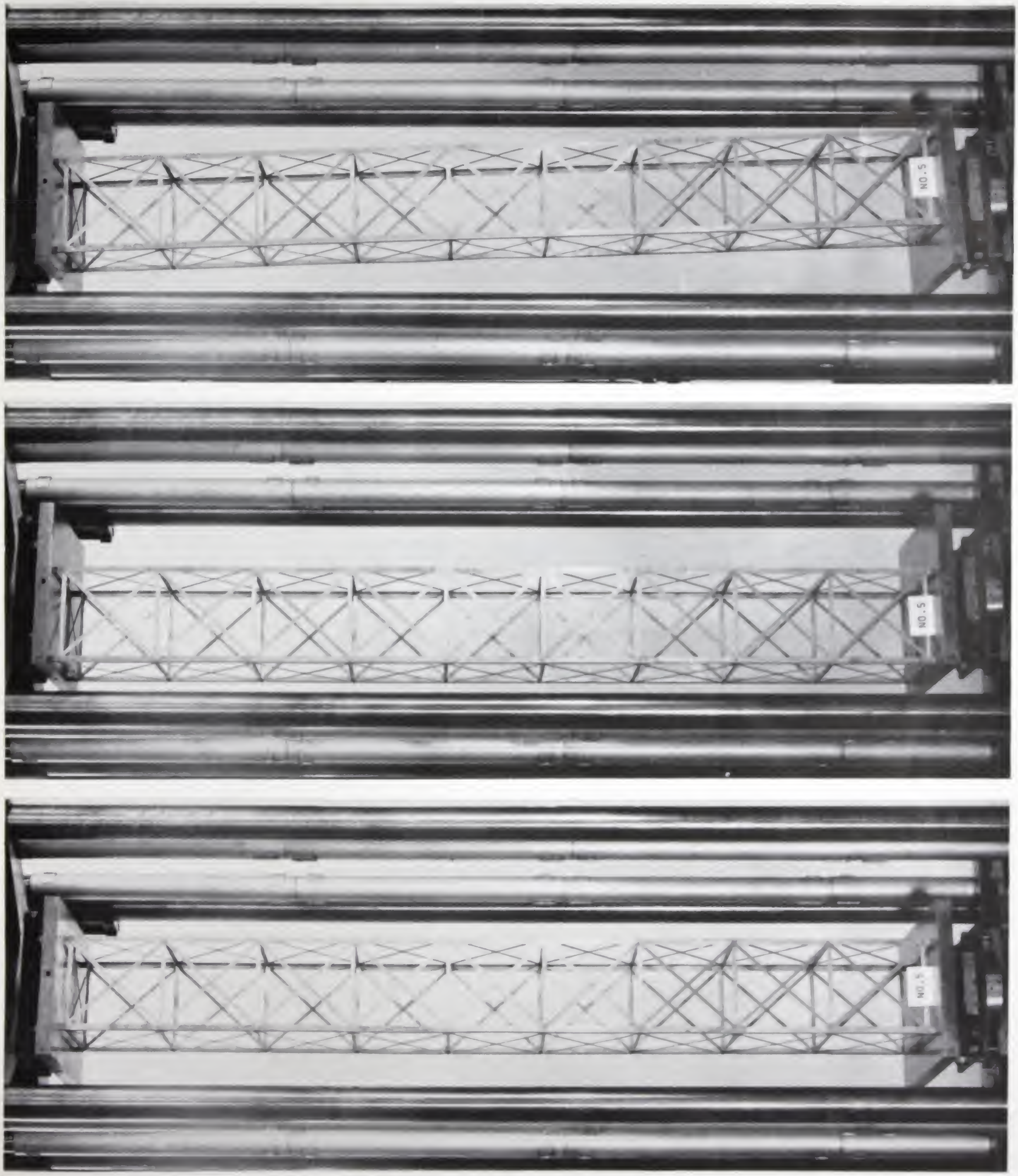

OBLIQUE LOAD

ECCENTRIC LOAD

AXIAL LOAD

FIGURE 3. COMPRESSION TESTS ON FRAME NO. 5.

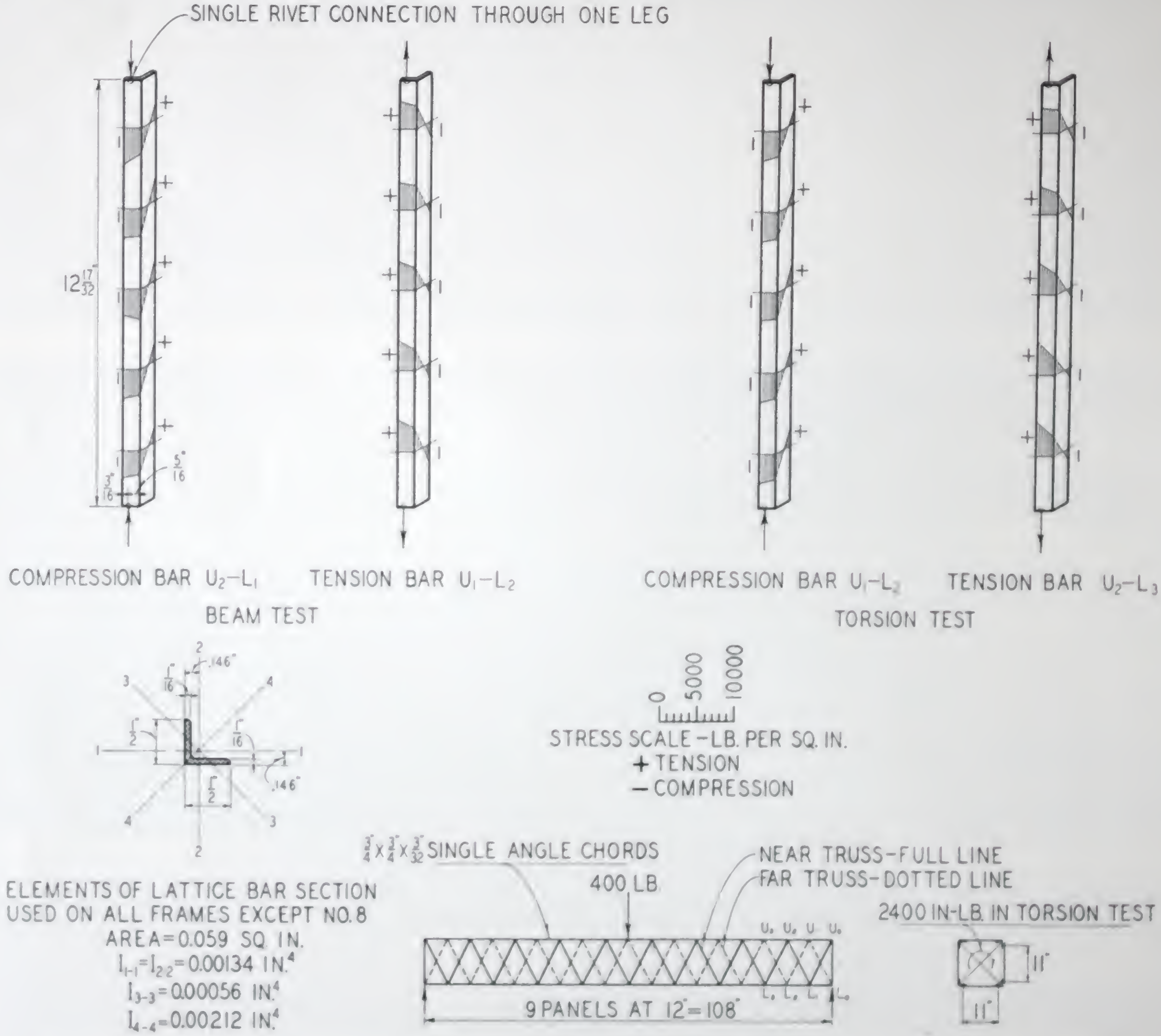

FIGURE 4. STRESS DISTRIBUTION IN LATTICE BARS OF FRAME NO. 1—BEAM AND TORSION TESTS.

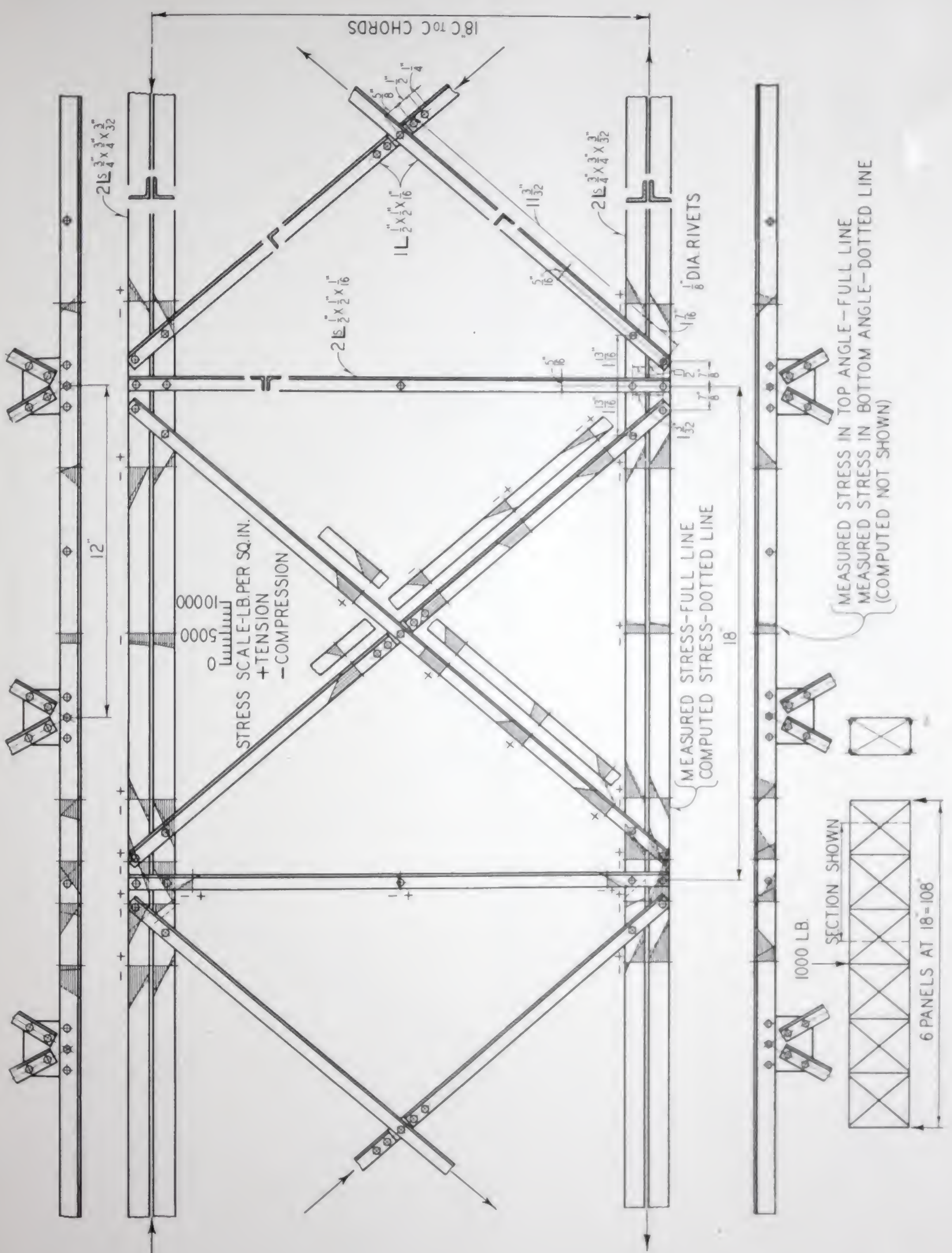

Figure 5. Stress Distribution in Frame No. 9—Beam Test.

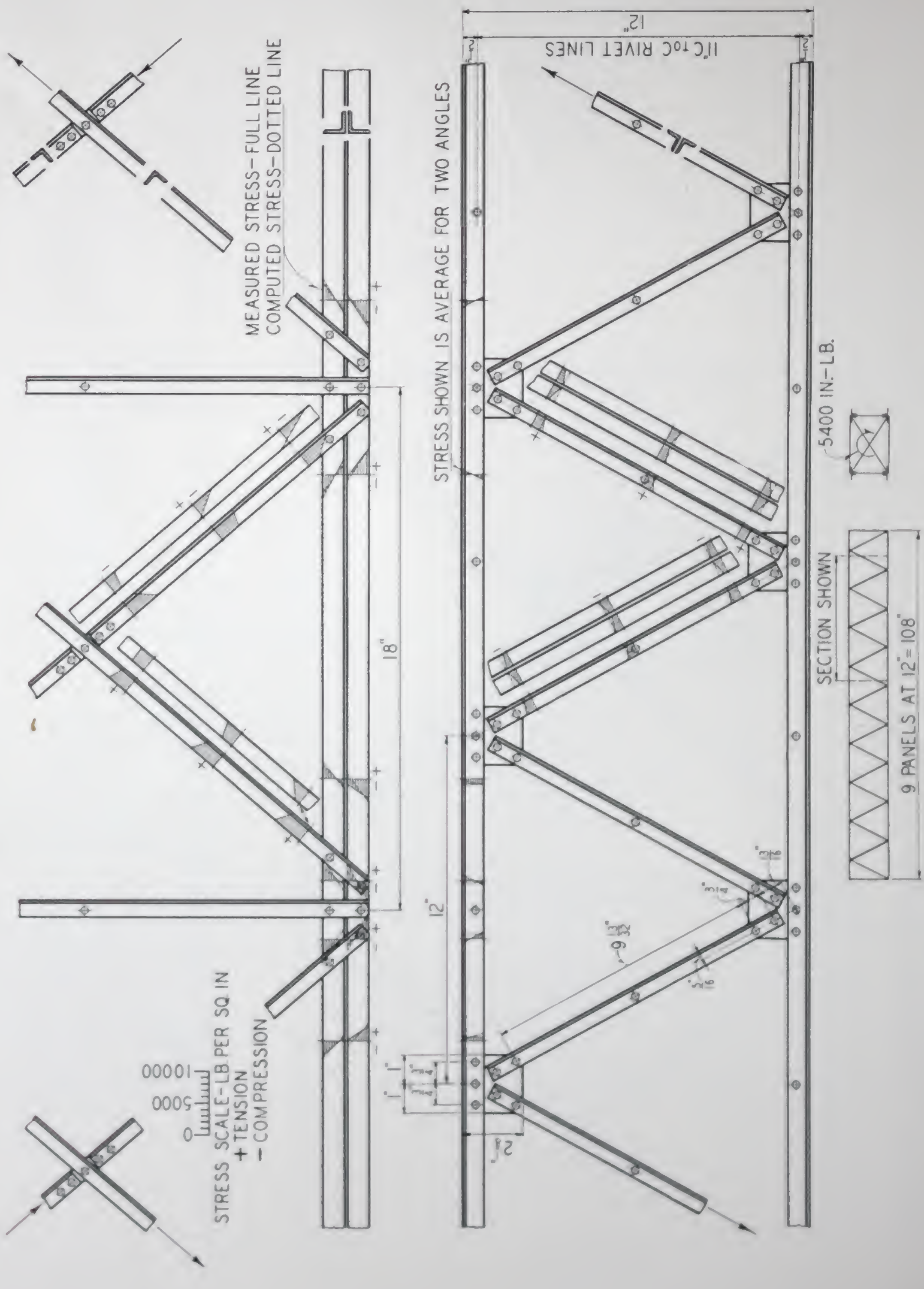

Figure 6. Stress Distribution in Frame No. 9—Torsion Test.

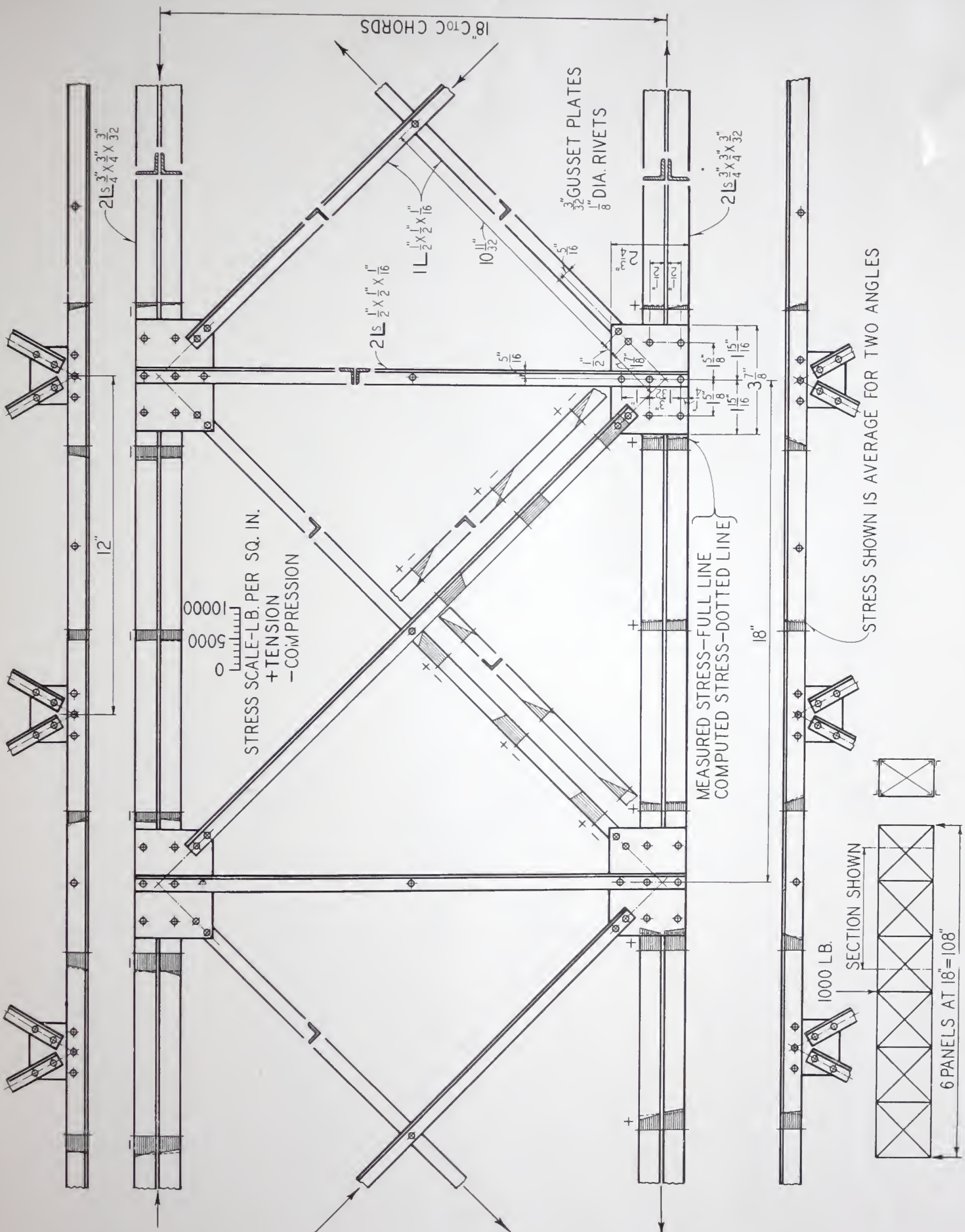

FIGURE 7. STRESS DISTRIBUTION IN FRAME NO. 10—BEAM TEST.

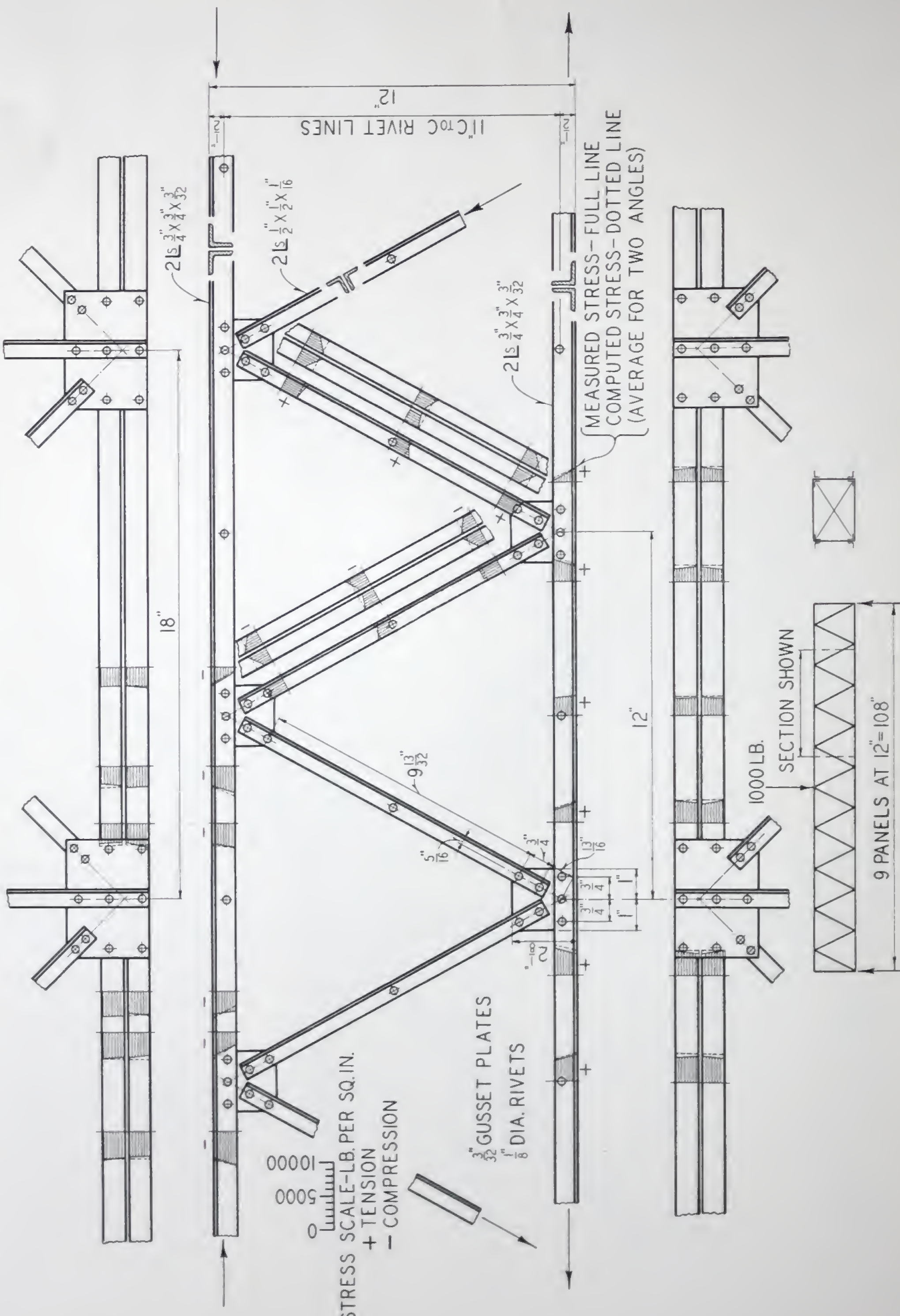

Figure 8. Stress Distribution in Frame No. 10—Beam Test.

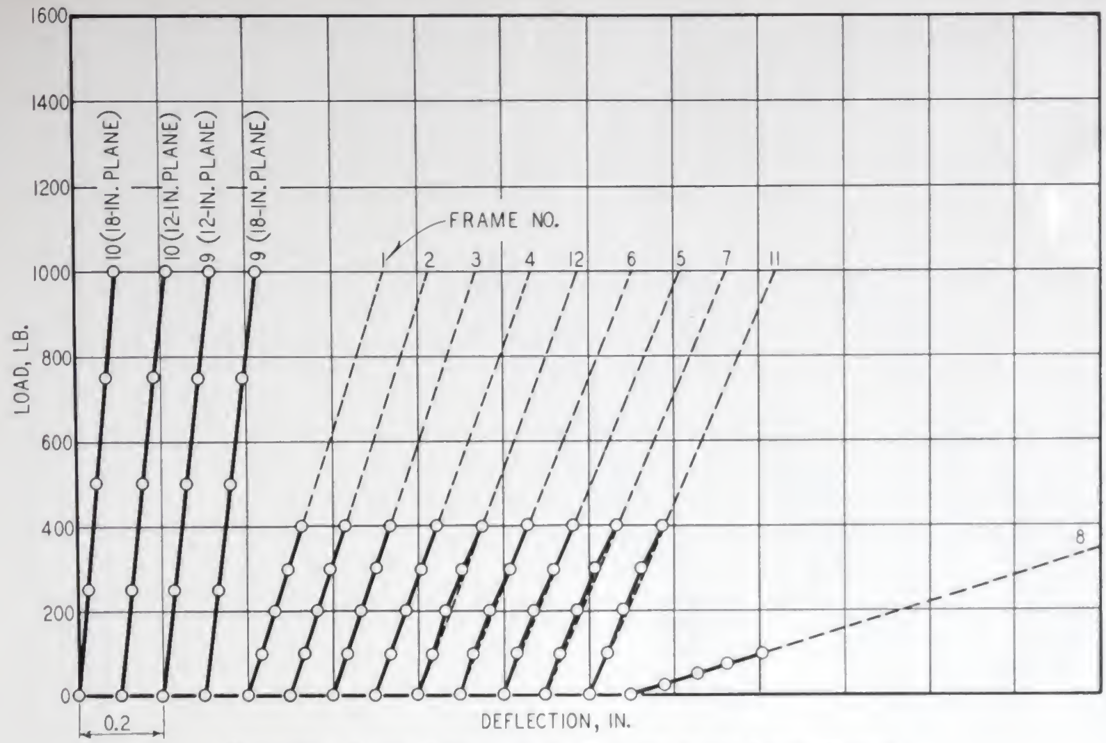

Figure 9. Load Deflection Curves from Beam Tests.

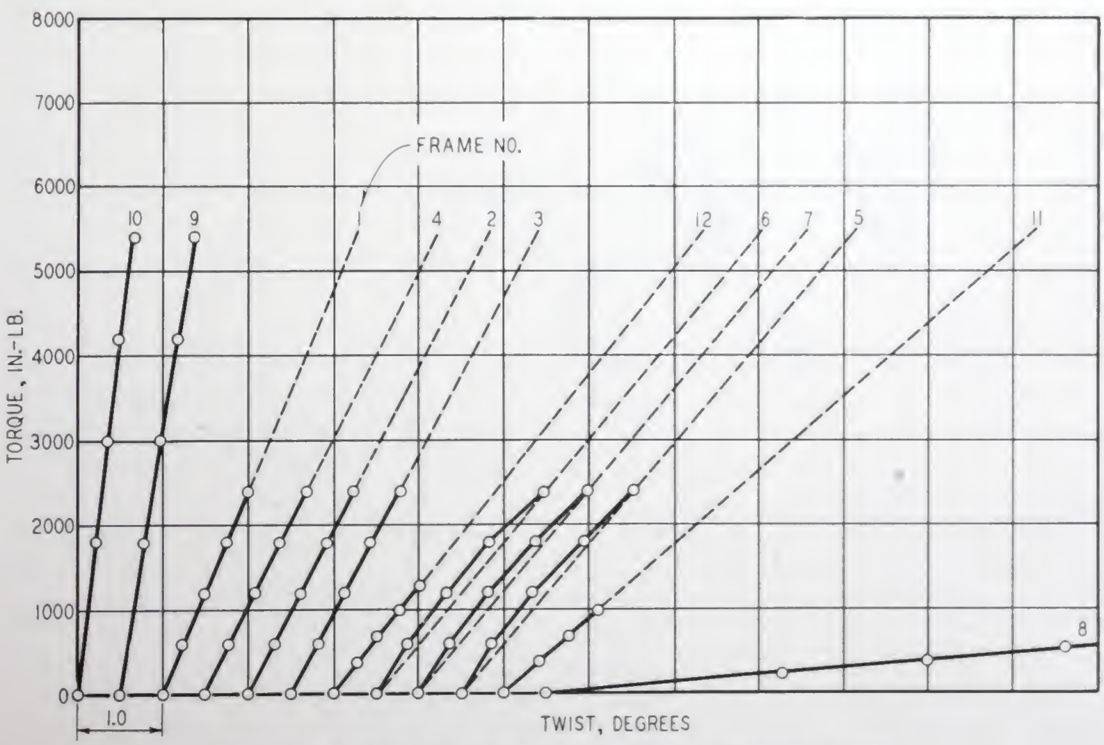

Figure 10. Torque-twist Curves from Torsion Tests.

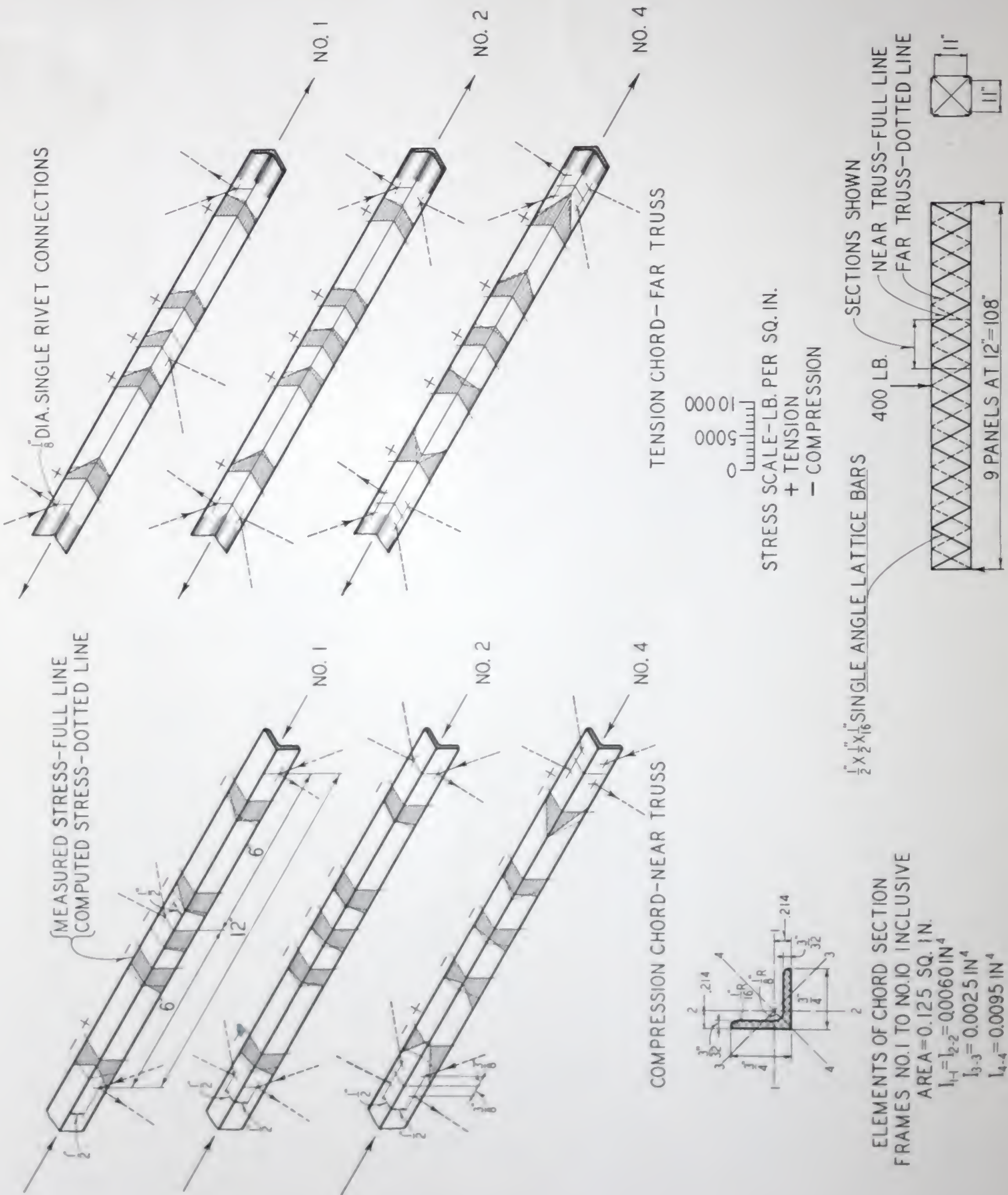

FIGURE 11. STRESS DISTRIBUTION IN CHORDS OF FRAMES NO. 1, 2 AND 4—BEAM TEST.

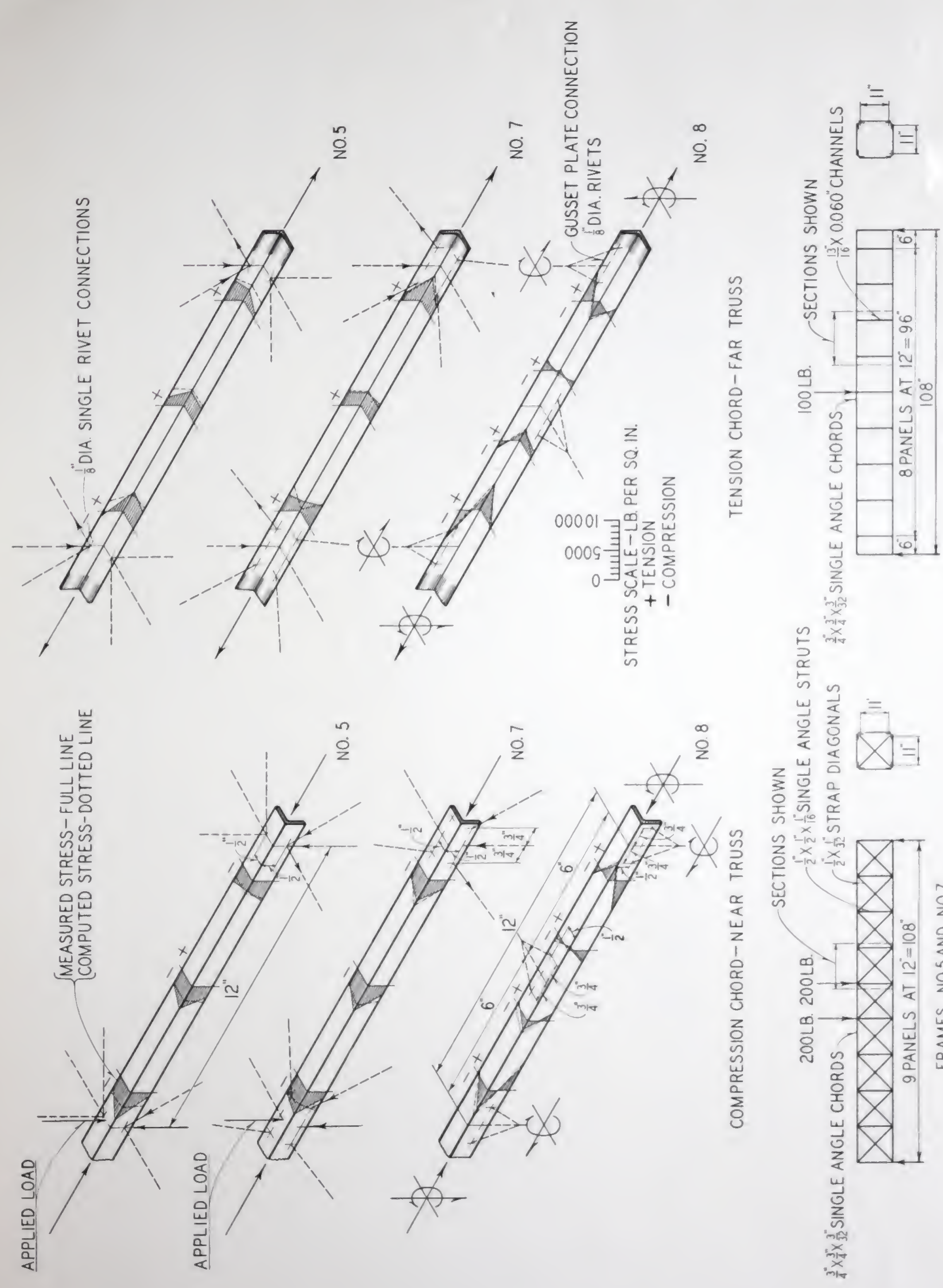

Figure 12. Stress Distribution in Chords of Frames No. 5, 7, and 8—Beam Test.

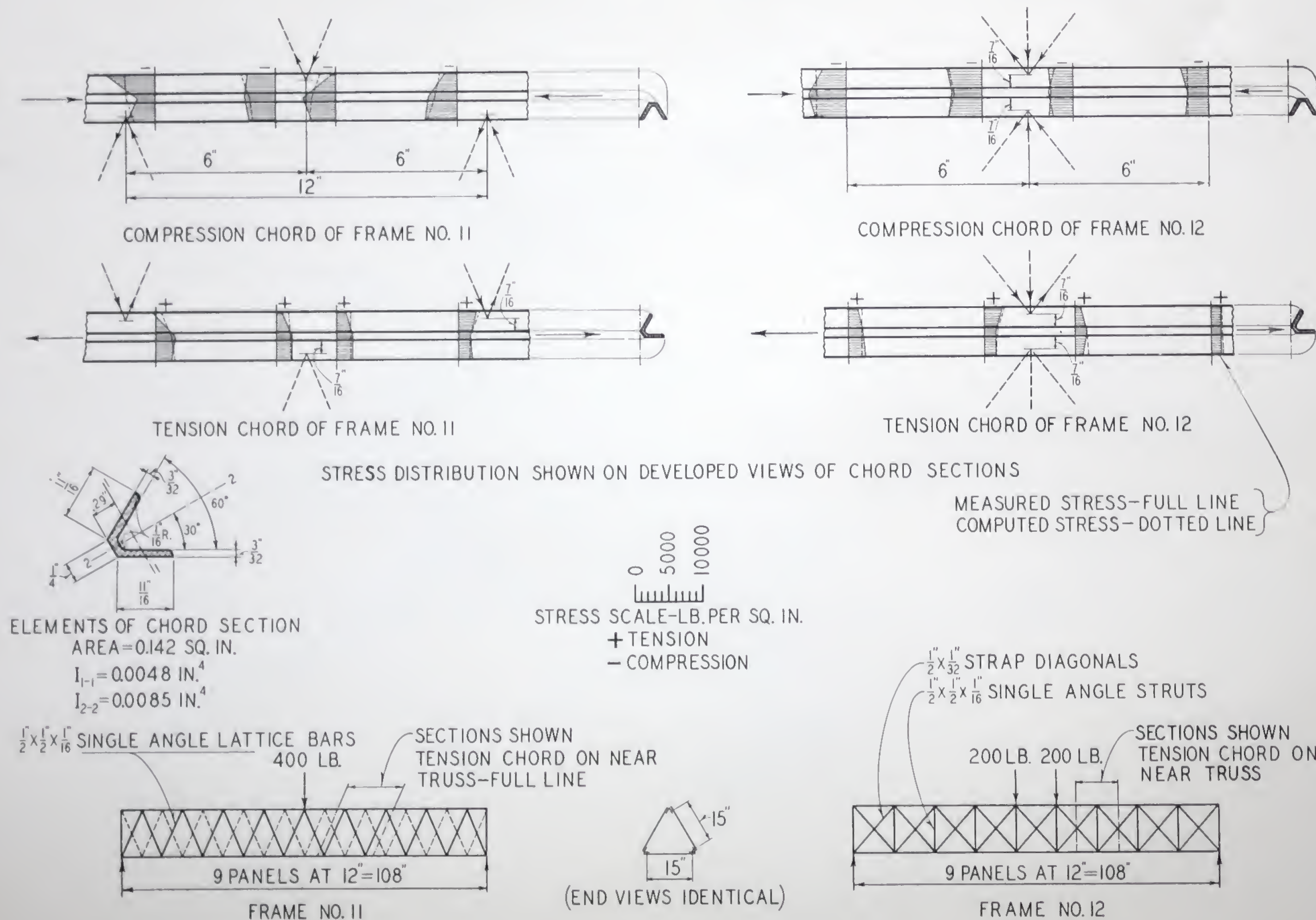

Figure 13. Stress Distribution in Chords of Frames No. 11 and 12—Beam Test.

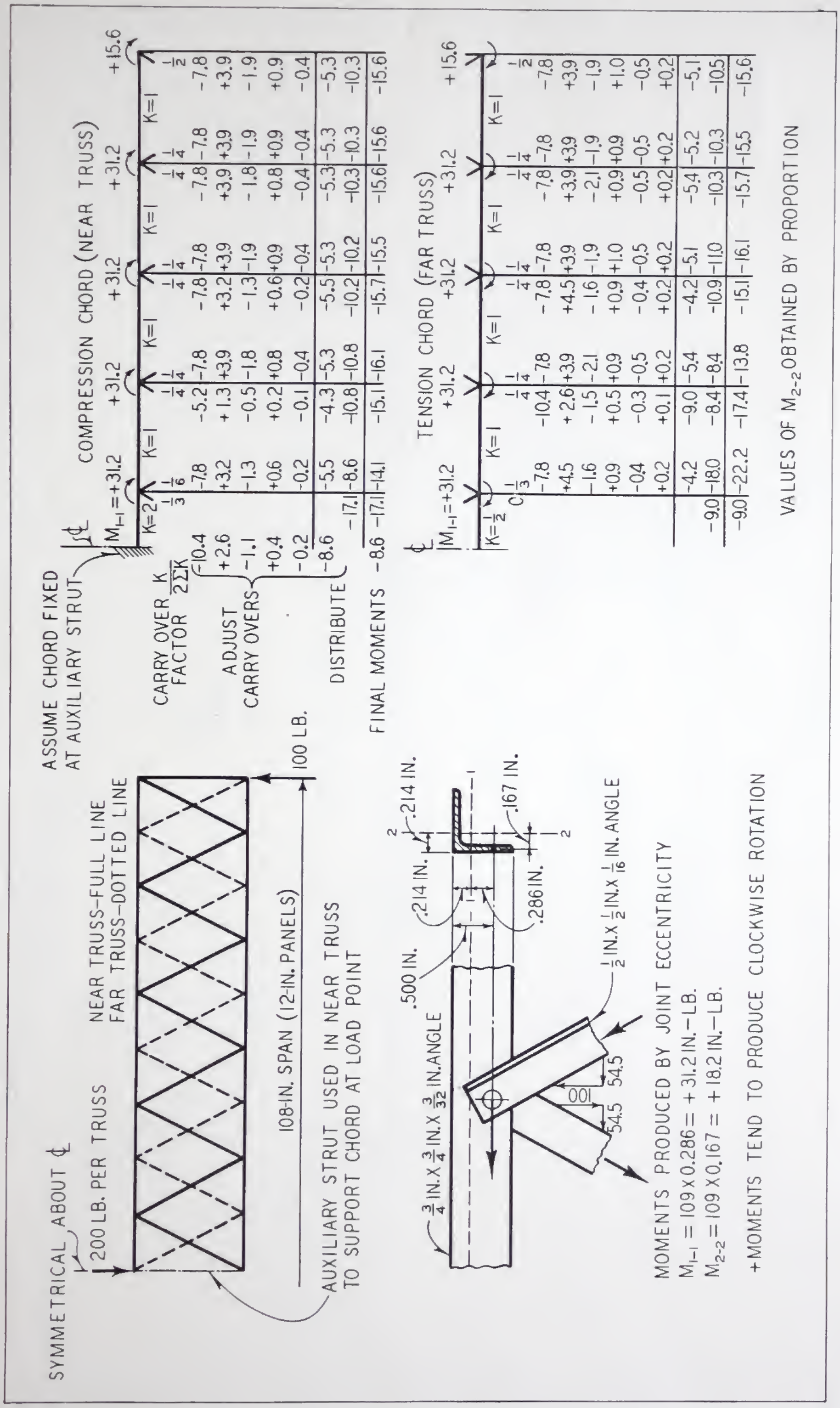

FIGURE 14. SECONDARY BENDING MOMENTS IN CHORDS OF FRAME NO. 1—BEAM TEST.

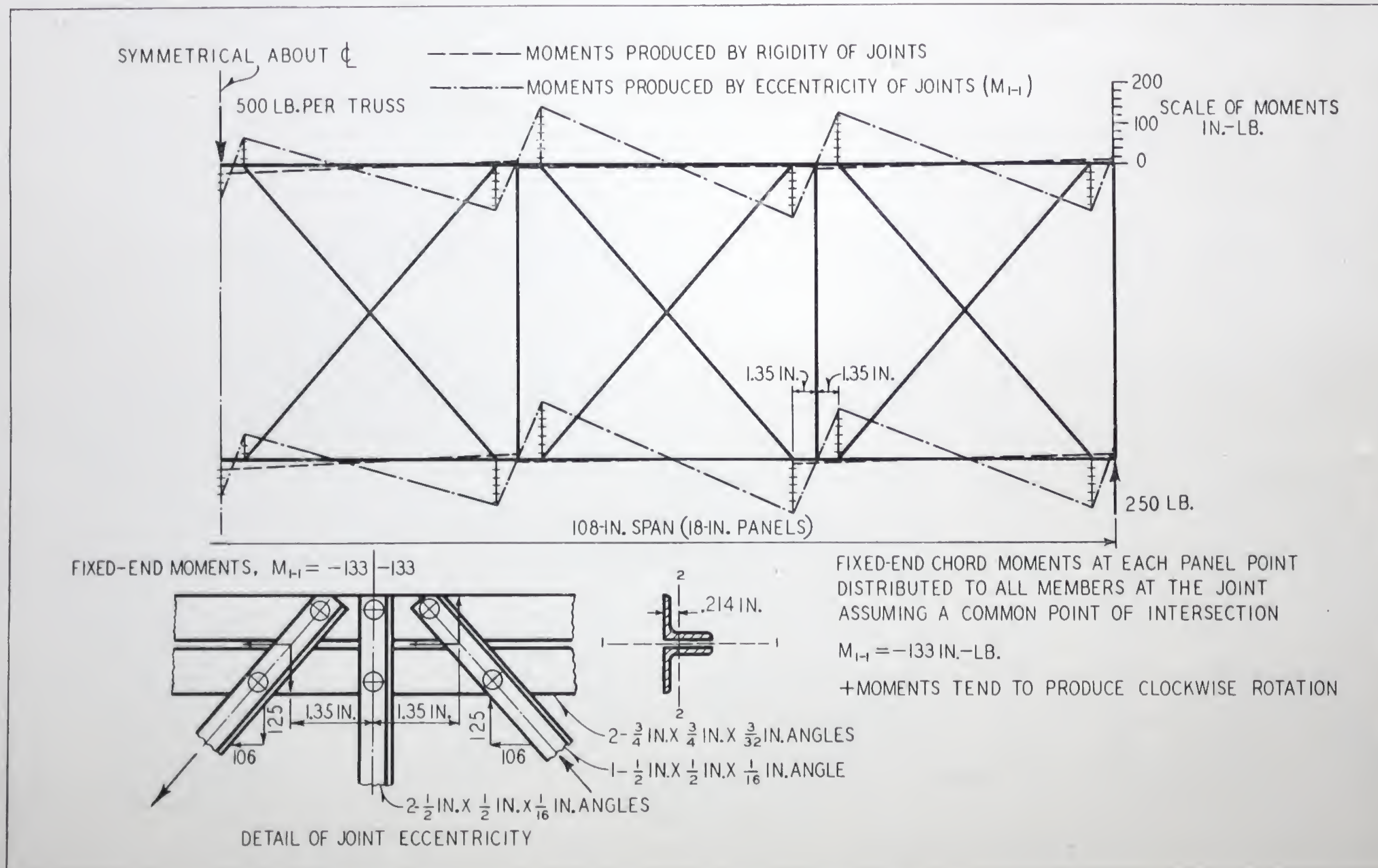

Figure 15. Secondary Bending Moments in Chords of Frame No. 9—Beam Test.

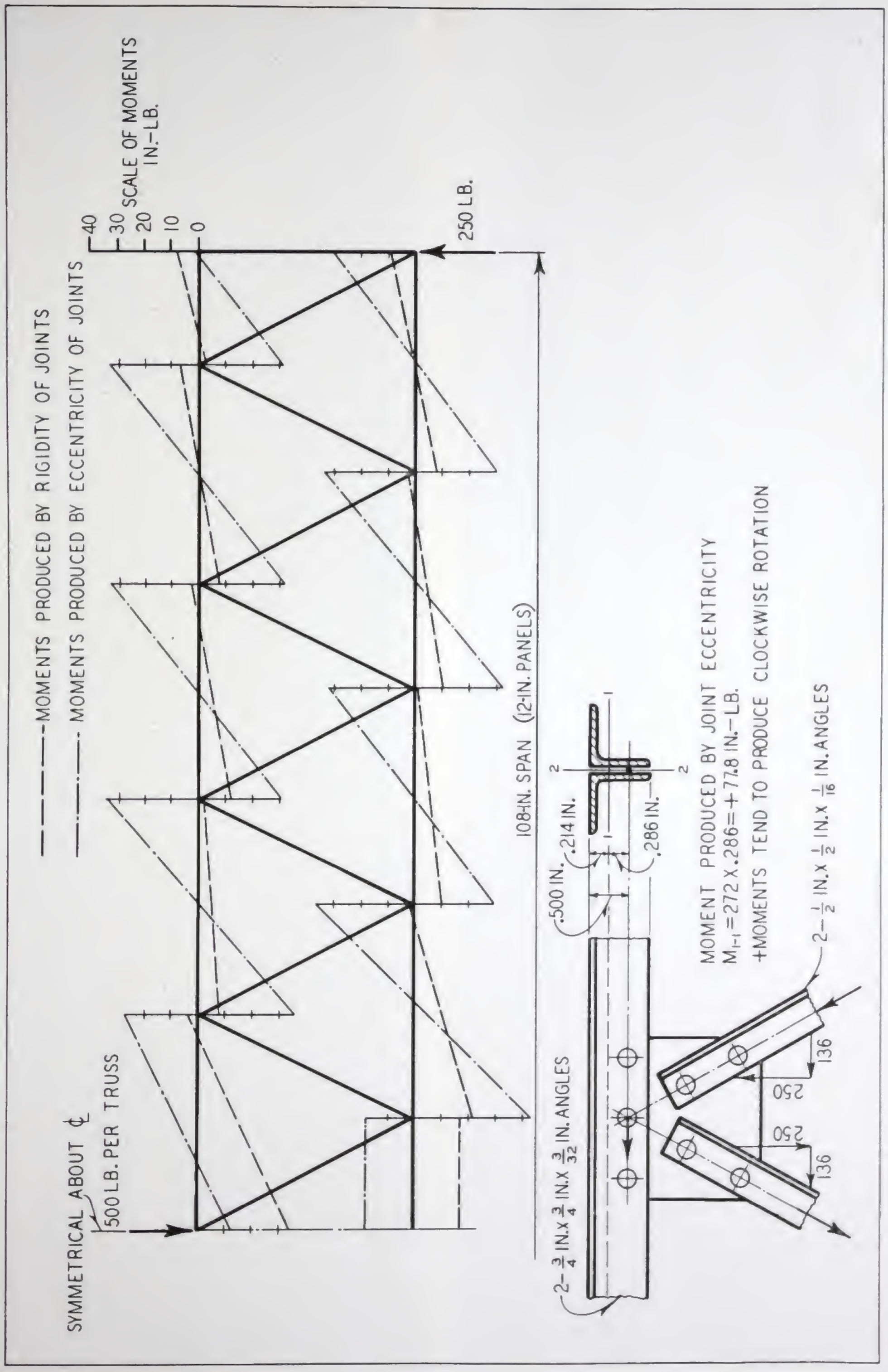

Figure 16. Secondary Bending Moments in Chords of Frames No. 9 and 10—Beam Test.

Figure 17. Frames No. 1 and 2 After Failure in Compression Test.

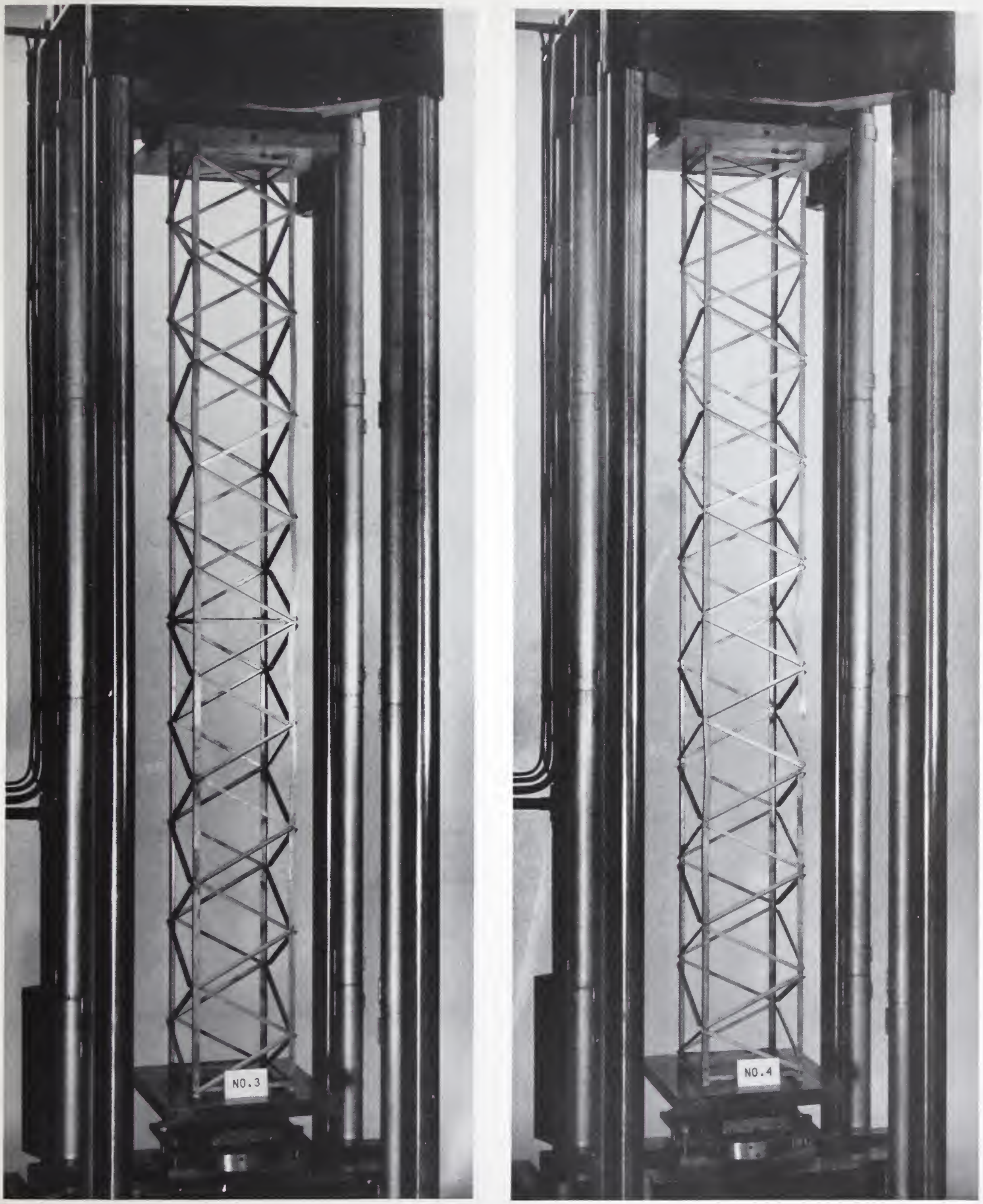

FIGURE 18. FRAMES NO. 3 AND 4 AFTER FAILURE IN COMPRESSION TEST.

FIGURE 19. FRAMES NO. 5 AND 6 AFTER FAILURE IN COMPRESSION TEST.

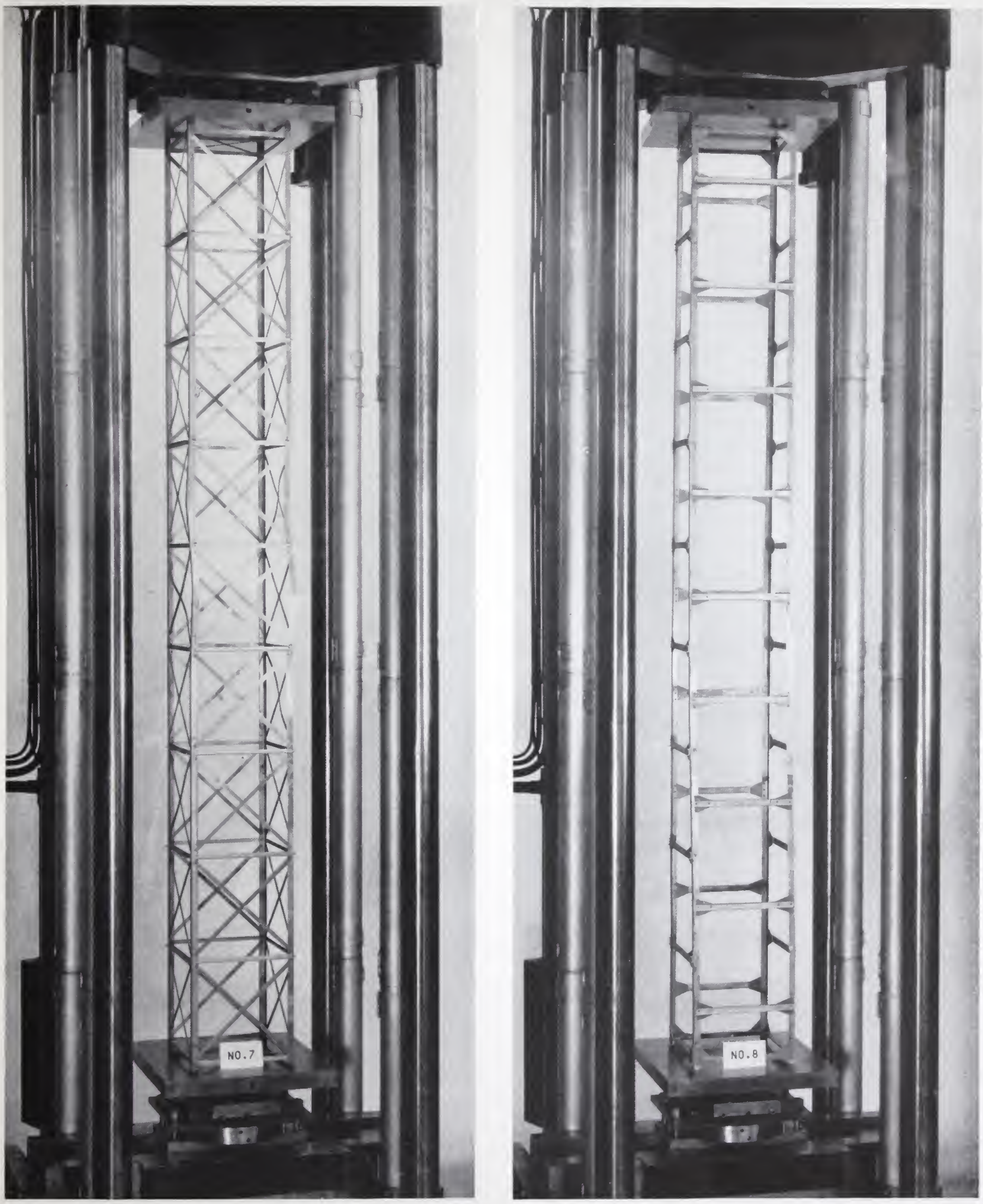

FIGURE 20. FRAMES NO. 7 AND 8 AFTER FAILURE IN COMPRESSION TEST.

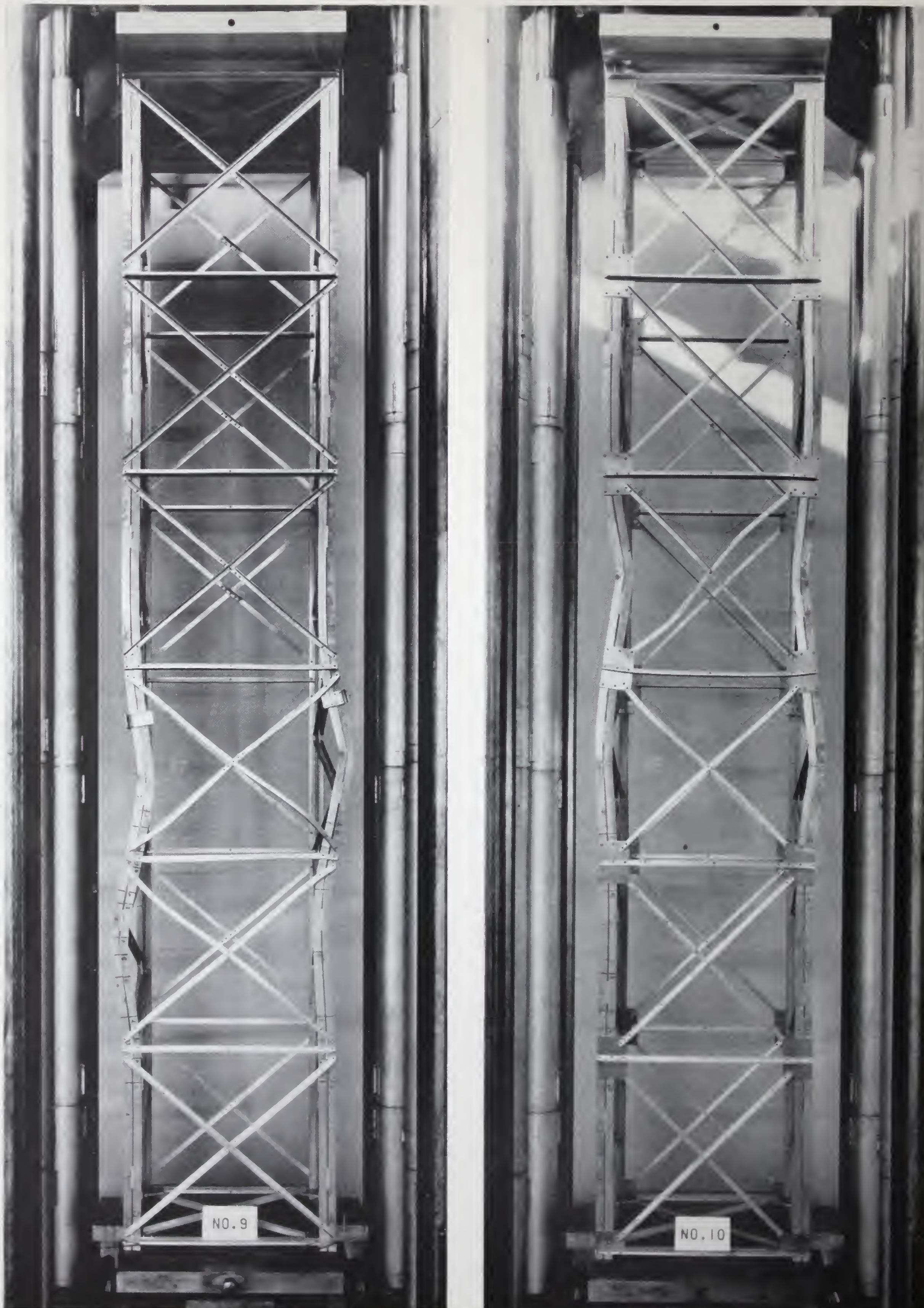

FIGURE 21. FRAMES NO. 9 AND 10 AFTER FAILURE IN COMPRESSION TEST.

FIGURE 22. FRAMES NO. 11 AND 12 AFTER FAILURE IN COMPRESSION TEST.

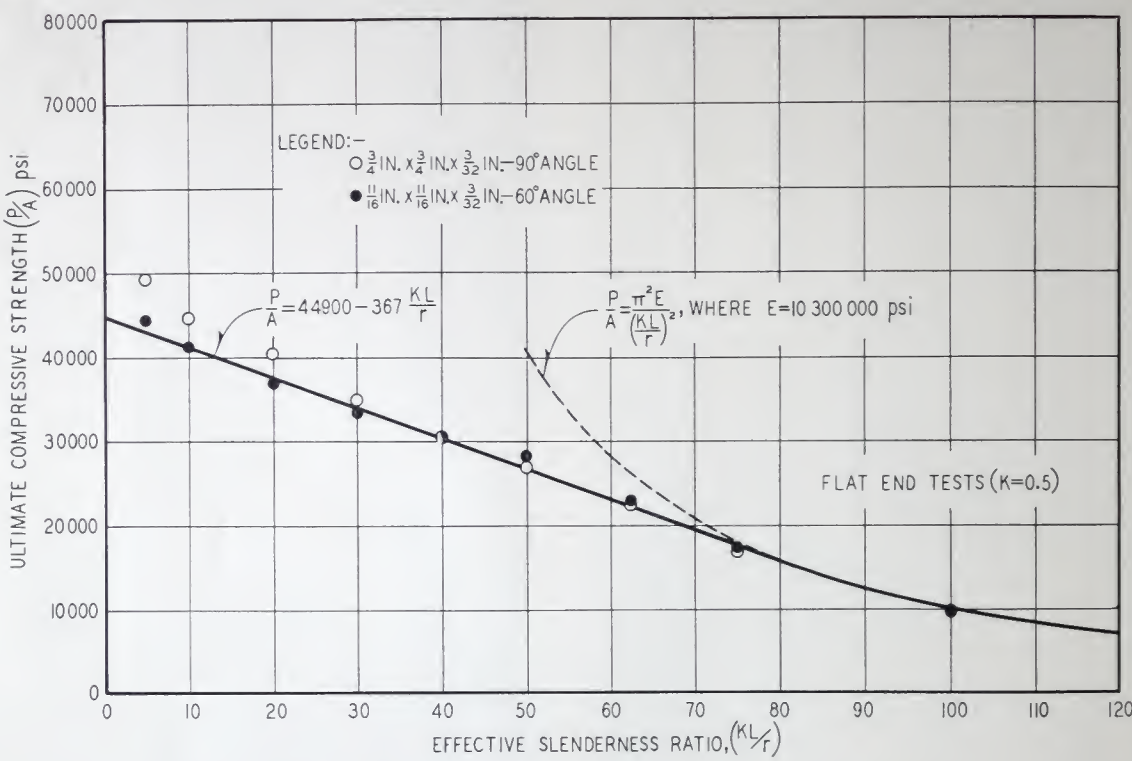

FIGURE 23. RESULTS OF COLUMN TESTS ON 17S-T CHORD ANGLES.

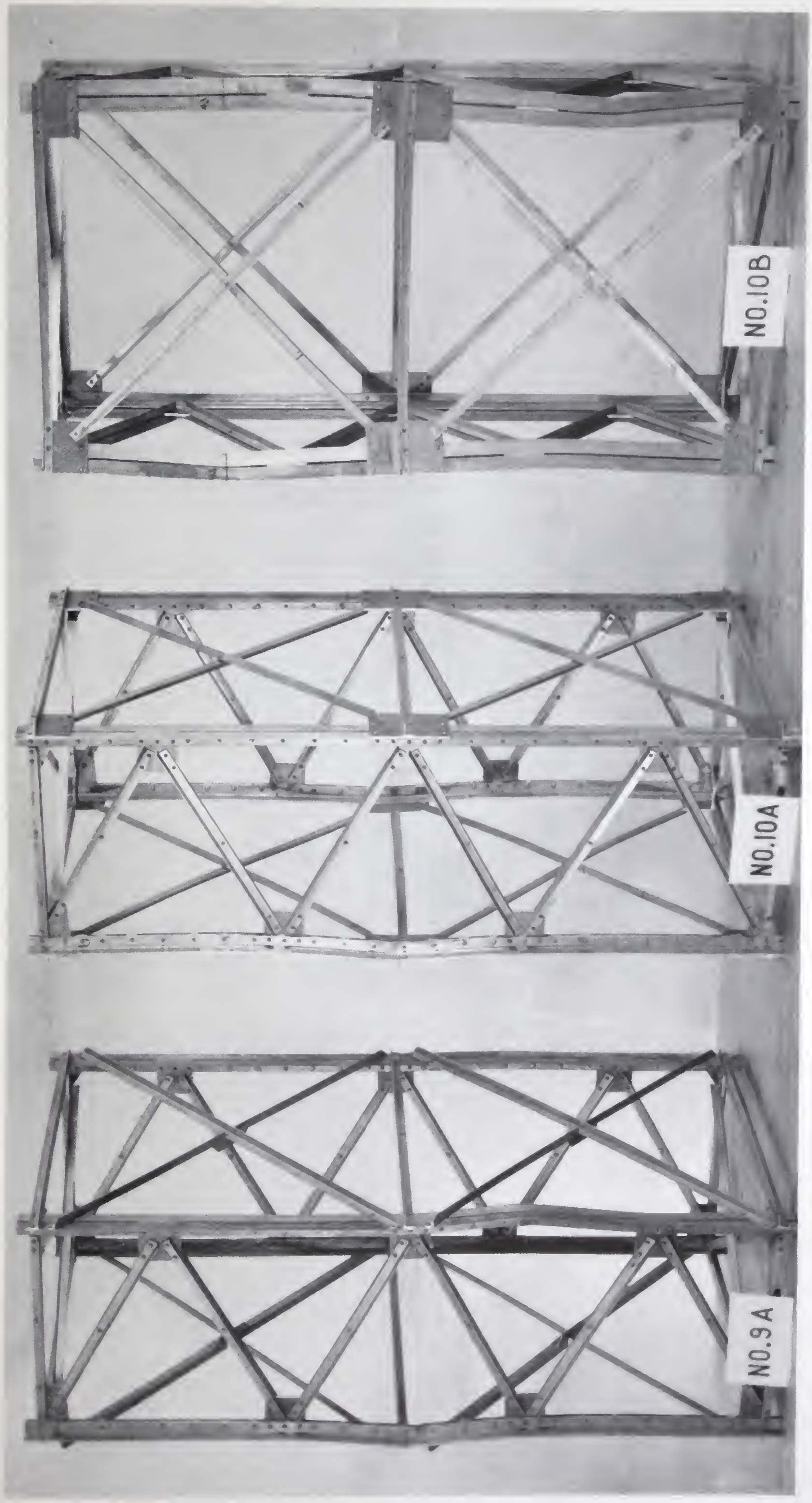

Figure 24. Frames No. 9A, 10A and 10B after Failure in Compression Test.